Development of Pharmaceutical VOCs Elimination by Catalytic Processes in China

Lilong Zhou [1,*, Chen Ma [1], Jonathan Horlyck [2], Runjing Liu [1] and Jimmy Yun [1,2,3,***

[1] College of Chemical and Pharmaceutical Engineering, Hebei University of Science and Technology, Shijiazhuang 050018, China; machen33@126.com (C.M.); liurj@hebust.edu.cn (R.L.)
[2] School of Chemical Engineering, The University of New South Wales, Sydney NSW 2052, Australia; j.horlyck@outlook.com
[3] Qingdao International Academician Park Research Institute, Qingdao 266000, China
[*] Correspondence: llzhou@hebust.edu.cn (L.Z.); jimmy.yun@unsw.edu.au (J.Y.)

check for updates

Abstract: As a byproduct of emerging as one of the world's key producers of pharmaceuticals, China is now challenged by the emission of harmful pharmaceutical VOCs. In this review, the catalogue and volume of VOCs emitted by the pharmaceutical industry in China was introduced. The commonly used VOC removal processes and technologies was recommended by some typical examples. The progress of catalytic combustion, photocatalytic oxidation, non-thermal plasma, and electron beam treatment were presented, especially the development of catalysts. The advantages and shortages of these technologies in recent years were discussed and analyzed. Lastly, the development of VOCs elimination technologies and the most promising technology were discussed.

Keywords: VOCs; catalytic combustion; China; elimination technology; pharmaceutical industry

1. Introduction

Recently, the Chinese public has become increasingly concerned about the levels of chemical air pollution present in the form of haze. A main contributing factor to this pollution is the release of volatile organic compounds (VOCs) from the industry. VOCs are organic compounds with boiling points in the range of 50–260 °C at atmospheric pressure or with a Reid vapor pressure of over 10.3 Pa at room temperature (293.15 K) and atmosphere pressure (101.325 kPa) [1,2]. The pharmaceutical industry is a major source of these VOCs [3,4], which can have serious ramifications, such as toxicity, carcinogenesis, mutagenesis, photochemical pollution, haze, and fog [5–9]. The pharmaceutical industry has developed greatly in China, as the production of bulk drug intermediates and Chinese patent drugs increased from 205,070 to 340,830 kilotons, and 112,890 to 374,600 kilotons in the past 10 years (2007–2016), respectively [10]. Meanwhile, the amounts of released VOCs increased from about 174.8 to 393.2 kt in the pharmaceutical industry [11,12]. The guiding emission standards of VOCs went into effect on 1 January, 2018 in China, which led to new imputes to upgrade VOCs elimination equipment and technologies in factories across China [13].

2. Catalogue and Emission Amounts of VOCs in the China Pharmaceutical Industry

2.1. Catalogue of Pharmaceutical VOCs in China

Medicines in China are mainly produced in six ways, biological fermentation, chemical synthesis, extraction, coagulation preparation, bioengineering, and treatment of traditional Chinese medicine [4,14]. The different methods produce varying levels of pollution, with the order of emitted VOCs being biological fermentation > chemical synthesis > extraction > bioengineering > treatment of

traditional Chinese medicine > coagulation preparation [15]. All these processes can be plagued by the need for high volumes of solvents, the consumption of large quantities of complex organic precursors, or the production of volatile byproducts. Some of the volatile organic compounds used or produced in these processes may be released into the atmosphere, which causes air pollution. The released VOCs primarily include alkanes, alcohols, ketones, aromatic hydrocarbons, halohydrocarbons, amines, esters, ether, aldehyde, carboxylic acid, and sulfur containing organic compounds [4,11,12,14,15].

Biological fermentation is often used to produce antibiotics, vitamins, and amino acids, via processes which include fermentation, separation, purification, and refinement [16,17]. The primary source of emitted VOCs are the solvents used in these processes, especially in the separation and purification steps. Additionally, H_2S is also produced as a byproduct in some fermentation processes.

The chemical synthesis technology is usually used for the production of medicine which can be used for prevention, cure, and diagnosis of the disease [18,19]. It contains the units to synthesize intermediates from raw materials, modify the structure of intermediates, purify the products, and dry the final products. The VOCs from this process comprise solvents and unreacted intermediates, which are more complex and often harder to be eliminated than those produced from the biological fermentation. These VOCs include heptane, toluene, xylene, methanol, n-propyl alcohol, isopropanol, phenol, aminomethane, dimethylamine, aminobenzene, cyclohexylamine, triethylamine, butyraldehyde, acetone, chloroform, chlorobenzene, etc.

Extraction involves the use of physical, chemical, and biological methods to separate a substance from a mixture. In the case of the pharmaceutical industry, extraction is carried out to separate organic compounds of interest from liquid solvents [16,20]. As a result, extraction processes require a large supply of solvents, including toluene, naphtha, methanol, ethanol, isopropanol, phenol, acetone, ether, acetic ether, diethylamine, dichloromethane, dichloroethane, chloroform, etc. VOCs are released during extraction mainly from the organic solvents used within the process.

The bioengineering method is a new way to produce some new medicines, via processes such as cloning antibodies, genetic engineering drugs, and genetic engineering vaccines [21]. The VOCs released from this process are similar to those of biological fermentation. These VOCs come from the solvents used within the process and as byproducts of certain reactions. They include n-hexane, methanol, ethanol, formaldehyde, acetaldehyde, formic acid, propanediol, acetone, aminoehtyl alcohol, acetonitrile, acetic acid, acetocaustin, N, N-dimethylformamide, phenol, butanone, 4-methyl-2-pentone, n-propyl alcohol, isopropanol, n-pentanol, isopropyl ether, isobutyl aldehyde, etc.

Another process of pharmaceutical production is the manufacture of traditional Chinese medicines or certain Chinese patent drugs [22]. As this is a traditional process which involves the use of only limited organic solvents to treat the natural animals and plants, the production of VOCs is limited. Hence, this process only emits a spot of VOCs, SO_2, and smoke.

Coagulation preparation involves the formation of larger particle agglomerates from fine particle suspensions. In the synthesis of pharmaceuticals, it is the process of mixing the active ingredients with helper constituents (often called coagulants) to produce a drug which has the desired particle size. The physical nature of the coagulation process means that the waste produced via this method is primarily a solid particle with little notable VOC production [4,14–16,22].

2.2. The Guiding Emission Standards of VOCs in China

The guiding emission standards of VOCs include six kinds of VOCs on the boundary of factories (Table 1) and four pollutant classifications with a total of 16 compounds in the areas surrounding workshops and installations (Table 2) [13]. These parameters are determined in 1 h by 3~4 samples for the average value. They are detected by the portable instruments or GC. These target VOCs are carcinogenic, odorous, and harmful organic compounds, which are mainly used as solvents and raw materials.

Table 1. The extreme emission value of volatile organic compounds (VOCs) on the boundary of factories and the highest concentration of selected VOCs allowed in 1 h for employees [13].

Pollutants	Limiting Value (mg·m^{-3})	The Highest Concentration of Selected VOCs Allowed in 1 h for Employees (mg·m^{-3})
Benzene	0.4	6
Formaldehyde	0.2	0.1
Trichloroethylene [a]	0.1	30
Dimethyl sulfate [a]	0.5	0.5
Dichloromethane [a]	4.0	0.5
Non-methane organic compounds	4.0	-
Ozone	20	0.26

a. They will be put into effect after the publication of national standards.

**Table 2.** The limiting value of specific pollutants in workshops and installations [13].

Classification	Pollutant	The Limiting Values (mg·m^{-3})	
		General Area	Key Area
Carcinogens	Trichloroethylene [a]	1	1
	Benzene	4	4
	Formaldehyde	5	5
Toxic substances	Phosgene	0.5	0.5
	HCN	1.9	1.9
	Acrolein	3	3
	Methyl sulfate [a]	5	5
	Cl$_2$	5	5
Photochemically active substances	Toluene	25	15
	xylene	40	20
	Dimethyl sulfoxide [a]	100	50
	Butylene oxide [a]	100	50
Other	NH$_3$	20	10
	HCl	20	10
	CH$_3$OH	50	30
	CH$_2$Cl$_2$ [a]	75	45

a. They will be put into effect after the publication of national standards.

2.3. VOCs Emissions in the Chinese Pharmaceutical Industry

China is the second largest producer of pharmaceutical products, only behind the United States of America. There are more than 1300 kinds of drug intermediates, 30 types of medicaments, and over 4500 pharmaceutical products made in China [23]. According to previous studies, the total VOCs emissions scaled linearly with the amount of final pharmaceutical products. [24]. The results showed that about 0.55 kg of VOCs were discharged to the atmosphere for the production of each 1 kg of final drug products.

The total VOCs emissions from the pharmaceutical industry increased by over 120% from about 174.8 kt in 2007 to 393.2 kt in 2016 (Figure 1) [12]. Although the VOCs emitted from the pharmaceutical industry only account for approximately 1.1% of China's total VOCs emissions, the absolute emission amount is very large. VOCs emitted from the pharmaceutical industry are potentially more harmful to human beings and ecosystems than the VOCs emitted from other sources. Compared with other emission sources, such as decoration, oil extraction and refining, catering, shoemaking and furniture manufacturing, the VOCs from pharmaceutical industries are more diverse with higher local concentrations and are harder to be eliminated.
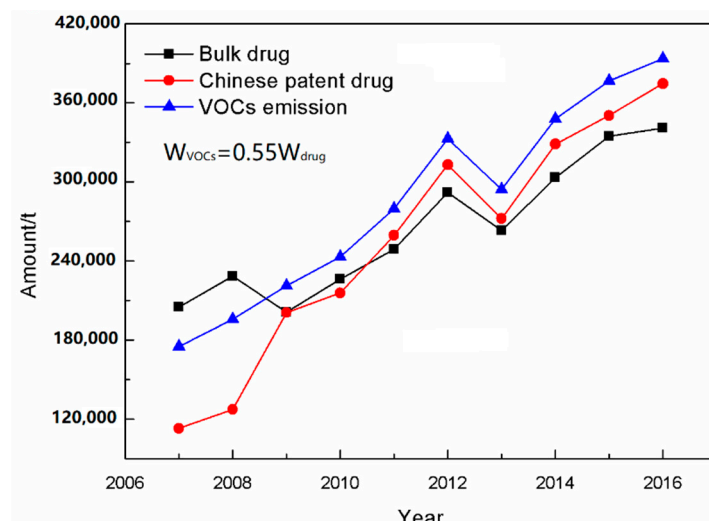
Figure 1. The production of bulk drugs and Chinese patent drugs and VOCs emissions from 2007 to 2016.

3. The Developing Technologies to Dispel VOCs

VOCs Elimination Technologies used in China's Pharmaceutical Industry

VOCs elimination technologies used in China were originally developed with the aim of recycling organic compounds to reduce cost, but recently the use and implementation of these technologies are targeted at minimizing the environmental impacts of VOCs. Technologies applied in the elimination of VOCs in China include condensation, absorption, adsorption, membrane purification, incineration, catalytic combustion, and the non-thermal plasma process (Figure 2) [15,25–27]. These methods are applied according to different working conditions, such as temperature and pressure, depending upon the VOCs targeted for removal. They also have distinct advantages and disadvantages. The development of these VOCs elimination technologies will be briefly introduced and discussed in this review. It is important to note that a wide range of VOCs which are often produced in a single waste stream and the various treatment technologies have different efficacies for the removal of certain VOCs. In fact, multiple technologies are often combined to eliminate the VOC mixtures from the waste streams.
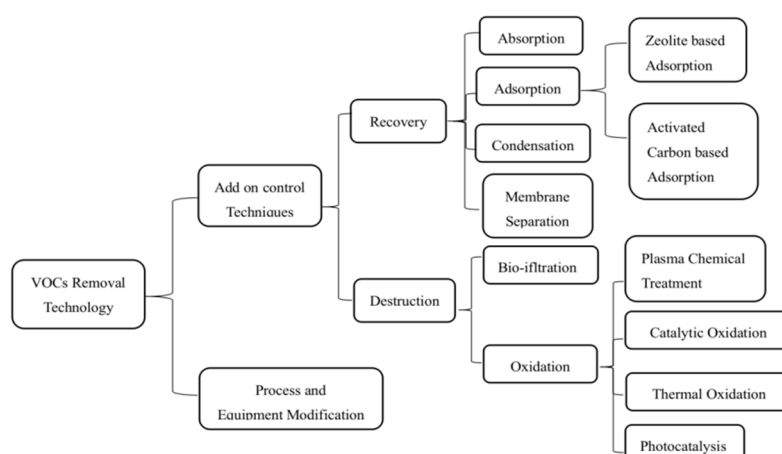

Figure 2. Classification of VOCs control techniques. Reprinted with permission from [26], 2000, Elsevier Ltd.

Condensation is the conversion of gas phase VOC mixtures with different vapor pressures to liquid via a decrease in temperature [28]. This technology is often used to recycle the solvents used in

pharmaceutical production, with the key advantages that equipment requirements and operation of the condensation process are simple. It makes the cost of condensation lower than other technologies. Another advantage is that the gas produced from condensation is pure. Hence, condensation is often used as the first procedure to treat the waste gas from a pharmaceutical workshop before incineration and absorption to reduce the load on more complex and expensive downstream technologies. Water and air are the most commonly used cooling mediums for the condensation process, but ice, cold salt solutions and organic mediums have been used where cooling temperatures below 10 °C are required, such as the $CaCl_2$ solution, NaCl solution, and ethylene glycol aqueous solution [4]. The condensation efficiency is sensitive to the temperature and pressure and is suitable for the removal of high concentration VOCs which exist as liquefied at moderate temperatures [29,30].

The removal of VOCs via adsorption involves the use of porous materials, while absorption utilizes solvents. The porous materials used in adsorption need a high absorption capacity, large surface area, good pore structure, stable chemical properties, high physical strength, and tolerance of acidic/basic conditions. The adsorption materials commonly used in this technology include activated carbon, porous silica, zeolite, and porous resin [31–35]. The solvents commonly used in the absorption of VOCs are water, acid solution, alkali solution, and other organic compounds [36]. The components used in the adsorption process include spray columns, filled towers, columns of trays, and washing apparatuses.

Both the adsorption and absorption methods have a high VOC removal efficiency and can almost completely remove VOCs from waste gas with low energy consumption (Figure 3). They can be used to recycle organic solvents and valuable compounds while remaining economically feasible. This technology is often used for the treatment of a large flow of waste gas with low VOC concentration in processes such as fix bed adsorption, moving bed adsorption, fluid-bed adsorption, and pressure swing adsorption [37–39]. Disadvantages of the adsorption and absorption process are also noteworthy, such as huge equipment requirements, complex procedures, and the need for desorption and regeneration of saturated absorbents. Due to its high overall VOC removal efficiency, this technology is commonly used in many pharmaceutical factories.
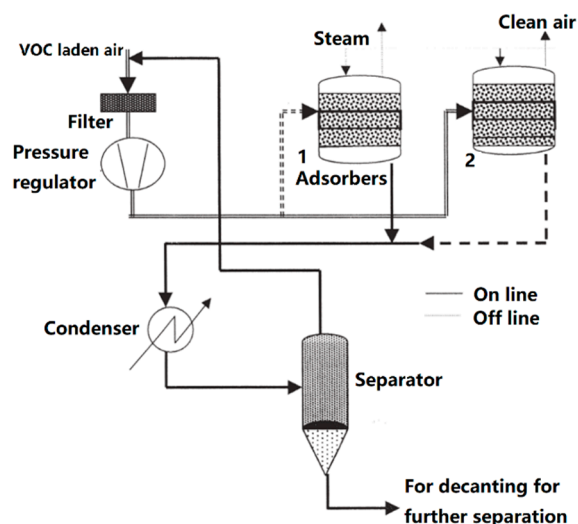
Figure 3. A typical activated carbon VOC removal (solvent recovery) plant. Reprinted with permission from [26], 2000, Elsevier Ltd.

Incineration is another widely used technology in pharmaceutical factories to eliminate VOCs (Figure 4). If VOC recycling is not technologically or financially feasible, incineration is a suitable method to completely eliminate VOCs [40]. Incineration is carried out by burning VOCs in a stove or kiln. Ideally, incineration results in the conversion of VOCs into CO_2 and H_2O in an efficient, simple, and safe manner. However, it has multiple shortcomings. If the VOCs concentration is too low to support the incineration, additional fuel is needed, which increases the running cost. Additionally,

some VOCs are less suitable for incineration, because the incomplete combustion of halogenated and other harmful VOCs can result in the release of toxic chemicals such as dioxin, NO_x, and CO [40].
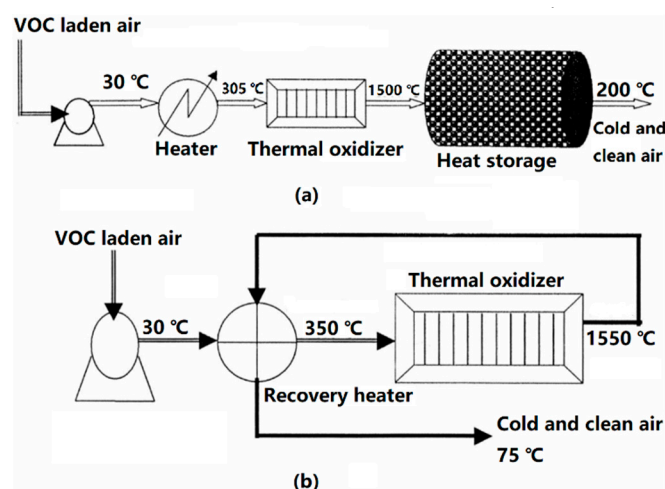
Figure 4. Schemes of thermal oxidation. (**a**) Regenerative thermal oxidation; (**b**) recuperative thermal oxidation. Reprinted with permission from [26], 2000, Elsevier Ltd.

To overcome the shortages of the incineration process for VOC destruction, the catalytic combustion technology was developed. In this process, VOCs are decomposed over catalysts at a low temperature (lower than 500 °C, Figures 5 and 6) [1,2,41–44]. The key factor which governs the catalytic combustion process is the activity of catalysts. Various kinds of catalysts have been used for the catalytic combustion of VOCs, such as noble metal catalysts, transition metal oxides, perovskite catalysts, and concentrated oxidation catalysts. The advantages for this technology are low operation temperature, decreased energy input requirements, high VOC removal efficiency, and minimal generation of toxic byproducts. Catalytic combustion is suitable for the treatment of waste streams containing VOCs across a wide range of concentrations. The main disadvantages of catalytic combustion are high investment requirements for equipment, short catalyst lifetime, and the need for process-specific designs, which are tailored to the waste stream. Nonetheless, the development of viable materials for the catalytic combustion process is still a hotspot for catalysis science.
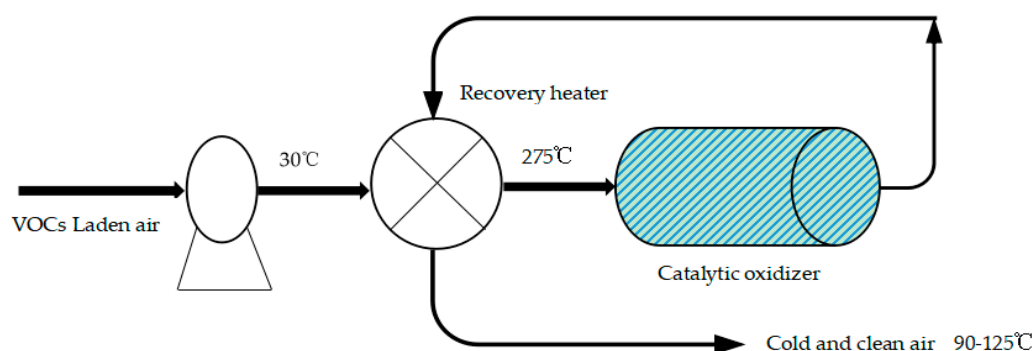
Figure 5. Scheme of catalytic oxidation. Reprinted with permission from [26], 2000, Elsevier Ltd.

The mechanism of catalytic combustion is considered by three types, with these being the Mars-Van Krevelen (MVK) model, Langmuir-Hinshelwood (LH) model, and Eley -Rideal (ER) model. In the Mars-Van Krevelen model, the VOCs molecules are initially adsorbed on the active sites, upon which they react with the oxygen species within the catalyst and are decomposed. Then, the reduced catalyst is re-oxidized by the supply of oxygen to the reactor. In the Langmuir-Hinshelwood model, the adsorbed VOCs molecules react directly with the adsorbed oxygen molecules, all occurring on the

catalyst surface. In the Elay-Rideal mechanism, the adsorbed oxygen reacts with the VOCs molecules in the gas phase. The reaction pathway which follows depends on both the catalyst materials and the target VOCs in individual systems.
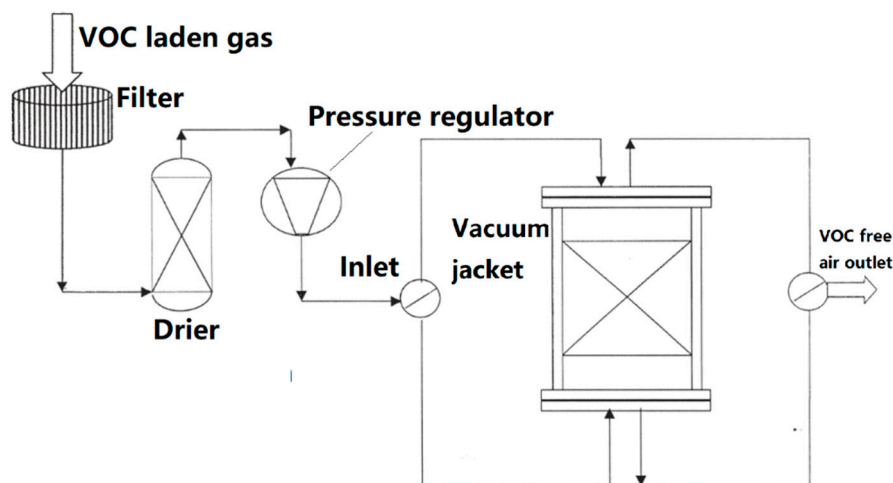
Figure 6. Schematic diagram of a reverse flow reactor. Reprinted with permission from [26], 2000, Elsevier Ltd.

Biodegradation is a widely used process for the treatment of pharmaceutical wastewater (Figure 7) [45,46]. It also can be applied to the treatment VOCs in the gas phase, especially for low concentration VOCs which are suitable for the growth of microorganisms. This process works with using the VOCs as a feedstock for the microorganisms, where they are converted to cytoplasm, CO_2, and H_2O. The sulfur and nitrogen elements in VOCs can be transformed to H_2S, nitrate, or N_2 at moderate temperatures. However, VOCs emitted from the pharmaceutical process often contain aromatics or halogens, which would poison the microorganism, rendering this method largely unviable in the abatement of pharmaceutical VOCs.
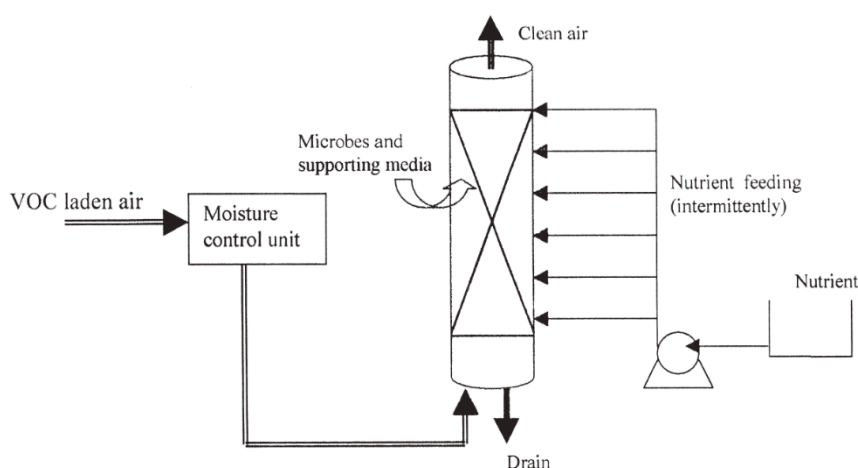
Figure 7. A simple schematic sketch of a bio-filtration system. Reprinted with permission from [26], 2000, Elsevier Ltd.

Non-thermal plasma is also a commonly used technology for the elimination of VOCs [47–49]. Free electrons and radicals formed during the plasma process react with VOCs and lead to the degradation of VOCs to CO_2 and H_2O. There are some advantages of the non-thermal plasma technology, such as a low press drop across the reactor, compact size, and simple equipment structure. The process can be started immediately without warm up and can treat VOCs with solid particles and liquid drops.

The non-thermal plasma technology can be combined with catalytic combustion to achieve a superior abatement of pharmaceutical VOCs.

The application of different VOCs elimination technologies depends on the factors such as the range and concentration of VOCs present in the waste stream, the volume of waste stream, and the funds available for installation and running costs. Jie Hao et al. summarized the scope of application for different VOCs elimination technologies (Table 3) [50]. Condensation and adsorption recycling are suitable for recycling VOCs. Catalytic combustion and incineration can remove the VOCs with a moderate concentration (3000–1/4 LEL) at high temperatures, while biodegradation and non-thermal plasma are suitable for abatement of low concentration VOCs at moderate temperatures. Hence, when selecting the efficient and economic VOCs abatement technologies, the scope of application for different technologies needs to be considered.

Table 3. VOCs elimination techniques and their operating conditions [50].

| Abatement Technologies	VOC Concentration $(mg \cdot m^{-3})$	Discharge Rate $(m^3 \cdot h^{-1})$	Temperature (°C)
Adsorption recycling	$100–1.5×10^4$	$<6 \times 10^4$	<45
Preheated catalytic combustion	3000–1/4 LEL *	$<4 \times 10^4$	<500
Thermal storage catalytic combustion	1000–1/4 LEL	$<4 \times 10^4$	<500
Preheated incineration	3000–1/4 LEL	$<4 \times 10^4$	>700
Thermal storage incineration	1000–1/4 LEL	$<4 \times 10^4$	>700
Adsorption concentration	<1500	$10^4–1.2 \times 10^5$	<45
Biodegradation	<1000	$<1.2 \times 10^4$	<45
Condensation	$10^4–10^5$	$<10^4$	<150
Non-thermal	<500	$<3 \times 10^4$	<80

* Lower explosive limit (LEL).

In a survey of 771 industrial applications of VOCs elimination processes, including 330 cases in China and 441 cases in various other countries (Figure 8), Jinying Xi et al. examined how often the various technologies were used [51]. The data showed that the most commonly used technology in China was adsorption (38%), followed by catalytic combustion (22%) and biodegradation (15%), while in other countries, the most often utilized were biodegradation (29%) and catalytic combustion (29%), followed by adsorption (16%). Due to its simple operation, low capital cost, and ability to recycle VOCs across a wide range of concentrations, adsorption was the most widely used technology in China. However, in some instances, the adsorption equipment was not well maintained and used correctly for recycling of VOCs. Adsorption, membrane purification, and condensation were the most effective methods, therefore most commonly applied, in instances where VOCs were present in concentrations above 10,000 $mg \cdot m^{-3}$. Catalytic combustion and incineration were used for the destruction of VOCs in the concentration range of 2000~10,000 $mg \cdot m^{-3}$, where recycling is not financially viable. Biodegradation and non-thermal plasma were applied for the treatment of VOCs in a lower concentration than 2000 $mg \cdot m^{-3}$. Some examples are introduced in the following section to illustrate the application of these technologies for the elimination of pharmaceutical VOCs in China [3,4,14,51,52].
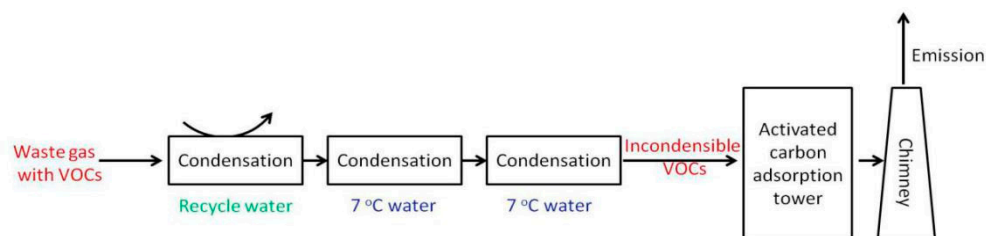
In the production of cefuroxime axetil, cefuroxime sodium, and cefotaxime sodium, the emitted VOCs include methanol, acetone, dichloromethane, DMF, acetic ether, and cyclohexane. One reported setup for the removal of these VOCs via a combination of condensation and adsorption technologies is described in Figure 9. Firstly, a portion of the various solvents was removed across a three-stage condensing unit comprised of a single stage of recycled water condensation, followed by two stages of 7 °C water condensation. The VOCs which were unable to be removed via the condensation process were removed by a two-stage activated carbon adsorption tower. The VOC-rich waste gas feedstock had a total VOC concentration of 2400 $mg \cdot m^{-3}$, of which 800 $mg \cdot m^{-3}$ was attributed to

methanol. It entered the first condensation unit at a rate of 2000 m$^3 \cdot$h^{-1}. More than 95% of the total VOC content was removed after the combined condensation and adsorption process. As a result, the emitted concentration and discharge rate of methanol was reduced to 18.9–29.3 mg$\cdot$m^{-3} and 0.08 kg$\cdot$h^{-1}, respectively, while the concentration and discharge rate of the other VOCs present was 55–63 mg$\cdot$m^{-3} and 0.16 kg$\cdot$h^{-1}, respectively. Both of these levels were in accordance with the emission standards of Hebei province where the factory was located.
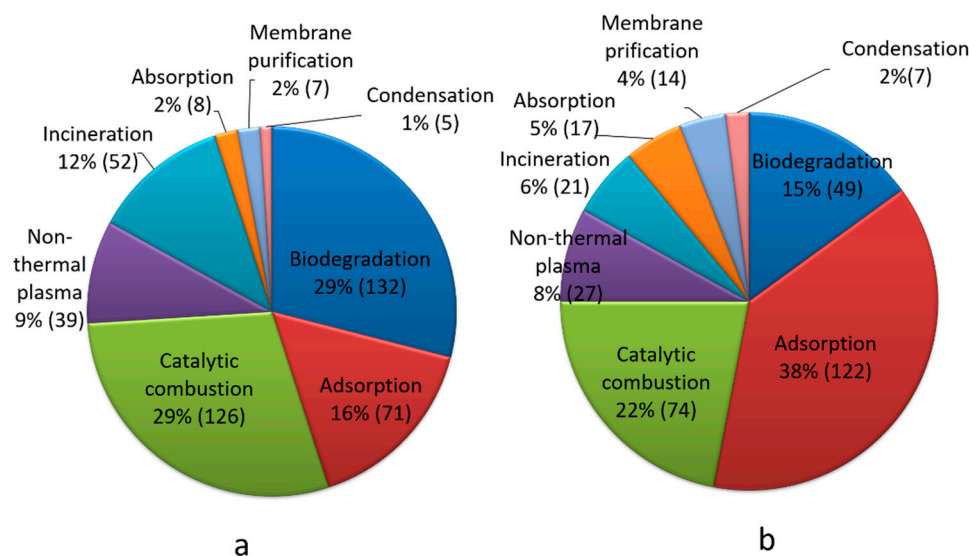
Figure 8. The ratios of VOCs elimination technologies used in China (**a**) and other countries (**b**) (the numbers in the brackets are the numbers of companies using the related technologies). Reprinted with permission from [51], copyright 2012, CNKI.


Figure 9. Representation of the VOC abatement process in a factory which produced cefuroxime axetil, cefuroxime sodium, and cefotaxime sodium. Reprinted with permission from [4], 2016, CNKI.

Yan Li has investigated the VOC abatement process in four separate companies in Taizhou city, Zhejiang province [4]. The main products in these four companies were clindamycin, clindamycin phosphate; losartan potassium, valsartan, nevirapine; meropenem, imipenem; and ciprofloxacin, spirolactone, respectively. There were three different procedures used in these four companies. The various procedures included adsorption, catalytic combustion, and non-thermal plasma technologies. The author assessed the efficiencies of the processes by measuring the concentration of a range of VOCs including benzene, toluene, xylene, methanol, formaldehyde, dichloromethane, chloroform, acetic ether, butylene oxide, acetonitrile, dimethylformamide, dysodia, and isopropanol before and after treatment. The results showed that after these elimination processes, the concentrations of VOCs in emitted waste gas were lower than the required concentration in standards for emissions of atmospheric pollutants from the pharmaceutical industry in Zhejiang province [53].

An example of a catalytic VOC treatment process is shown in Figure 10 below, which uses a regenerative catalytic oxidizer. The waste gas from the workshop was collected and combined with the waste gas from the sewage station, storehouse, and solid waste pile. The gas mixture was first washed with a water and alkali solution, then dehydrated and defogged. The dry gas was filtered, then heated

with a preheater with an attached regenerative heat transfer. The preheated gas mixture entered the catalytic reactor and was combusted. After catalytic combustion, the gas was washed again with a water and alkali solution and emitted to high altitude atmosphere by a fan. The removal efficiencies of dysodia and non-methane hydrocarbons were 68.07% and 94.33%, respectively. The running fee of the whole VOCs elimination system was about RMB 1 million per year.
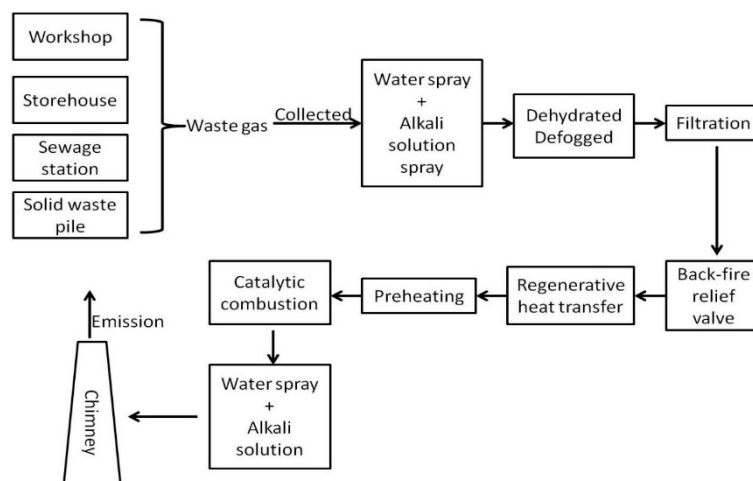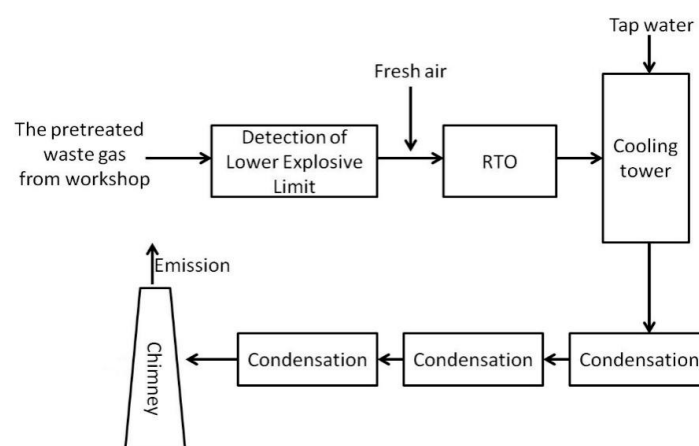

Figure 10. VOCs abatement process in the A factory. Reprinted with permission from [4], 2016, CNKI.

Two companies used a process which combines a regenerative thermal oxidizer (RTO) with three condensation stages connected in a series (Figure 11). The waste gas was pretreated in the workshop below determining the lower explosion limit (LEL) of the mixture. Then, fresh air was added in accordance with the determined LEL, such that the proper fuel, oxygen ratio, would be present in the RTO. After that, the gas mixture was oxidized in the RTO at a temperature of 850 °C with 98% of the thermal energy recycled. The high temperature gas exiting the RTO was cooled in a cooling tower, then further cooled across a three-stage condensation setup before it was emitted to the atmosphere. The dysodia concentration in the total vent was 300 mg·m^{-3}, while the concentration of non-methane hydrocarbons was lower than 85 mg·m^{-3}. These concentrations correspond to removal rates of 89% and 92% for dysodia and non-methane hydrocarbons, respectively. The main drawback of this procedure was that the condensation step was not effective for dichloromethane recycling and a lot of HCl generated from the incineration of chlorinated organic compounds, which in turn led to the corrosion of the equipment.

A process which combines the non-thermal plasma and catalytic oxidation techniques (oxidation of VOCs by H_2O_2 in a low pH) to treat VOCs in waste gas is outlined in Figure 12. The waste gas, with a high VOC concentration, was pretreated, combined with exhaust gas, and washed with an alkali solution. Then, the washed gas entered the catalytic combustion/oxidation tower, where a portion of the VOCs content was oxidized to CO_2 and H_2O. The oxidized waste gas was washed with water and entered a dehydrator to remove humidity. After that, the waste gas from the sewage station was added to the treated gas, upon which the gas mixture was treated with a non-thermal plasma, to remove additional VOCs. The gas was dehydrated again and entered into the second catalytic oxidation tower. The gas was washed by the alkali solution again and emitted to the atmosphere. The dysodia concentration was reduced by 84% to no more than 250 mg·m^{-3}. The removal efficiency of non-methane hydrocarbons content was approximately 92%, with a concentration of less than 85 mg·m^{-3} in the emitted gas.

These procedures (Figures 9–12 Figure 9 Figure 10 Figure 11 Figure 12) are representative of the range of VOCs elimination technologies currently in use in China. Almost all kinds of VOCs abatement technologies have been applied in the treatment of waste from the Chinese pharmaceutical industry. While the application of these technologies has successfully decreased the emission of VOCs, the

high cost of investment and low efficiency are still the main factors which hinder the application of these technologies in the industry. The adsorption, absorption, and biodegradation technologies face challenges concerning the production of secondary pollutants, the desorption of adsorbed VOCs, and the production of waste water and sludge. The incineration process is effective in removing the issue of secondary waste production, but it requires a large energy input and has safety risks posed by the high temperature and use of a flame within a factory. The catalytic combustion and non-thermal plasma technologies partially circumvent the issues of waste and high temperature, but they are currently costly techniques with a short equipment lifetime. Thus, the continuing improvement of these technologies and development of new technologies is needed. With the new emission standards/law coming into effect, VOC elimination processes need to be upgraded in many Chinese pharmaceutical factories. As such, there is a desire for novel, effective, and energy efficient technologies in the near future.

Figure 11. VOCs abatement process in the B and C factory, utilizing a regenerative thermal oxidizer (RTO) and condensation. Reprinted with permission from [4], 2016, CNKI.
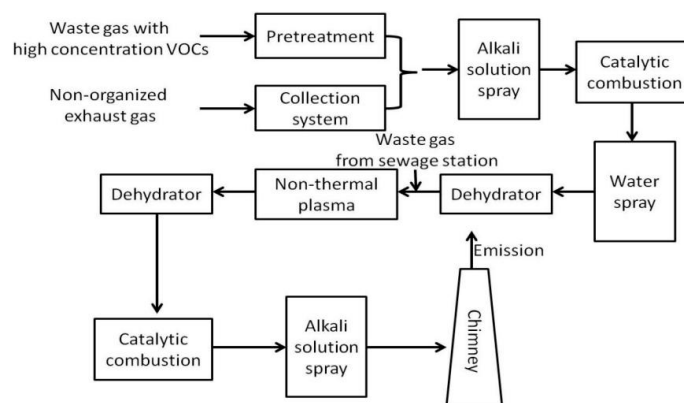
Figure 12. VOCs abatement process in the D factory. Reprinted with permission from [4], 2016, CNKI.

4. The Developing Technologies for VOCs Elimination

As outlined in the previous section, the VOC abatement technologies currently in use in China are hindered by some key limitations, such as high construction and running costs, low removal efficiencies for complex VOCs, and high temperature or energy requirements. To address these shortcomings, significant research is being carried out to improve the traditional methods of VOC removal, such as adsorption, catalytic combustion, and non-thermal plasma [1,2,33,41,43,44,47–49,54]. In addition, new technologies which can avoid the disadvantages of the traditional technologies have emerged, such as photocatalytic oxidation, condensation-oxidation, and electron beam treatment [2,42,48,55]. A summary of the various catalysts and conditions that have been investigated as active materials for the catalytic oxidation of VOCs is contained in Table 4 below.

Table 4. Reported catalysts for VOCs elimination.

VOCs	Refer	Catalyst	Catalytic Performance	Remarks	Catalytic Mechanism
Benzene	[56]	0.3% Pt/γ-Al$_2$O$_3$	T$_{95}$: 220 °C	-	-
	[57]	Pd-AuFeCeIM	T$_{100}$: 200 °C	-	-
	[58]	Layered copper manganese oxide (LCMO)	T$_{50}$: 218 °C T$_{90}$: 240 °C	The introduction of water vapor had no significant effect on the catalyst. The catalyst activity decreased about 30% after SO$_2$ was added. The addition of CO$_2$ has no effect on the catalytic activity of the catalyst.	The larger surface area and the formation of Cu^{2+}-O^{2-}-Mn^{4+} entities at the interface between CuO and layered MnO$_2$ promoted the CO and VOCs oxidation.
	[59]	LaCoO$_3$	T$_{50}$: 330 °C	Water vapor has no significant effect on the catalytic performance of catalyst.	Factors improve activity: (i) The larger exposed surface, (ii) the composition of the support provides increased oxygen mobility.
	[60]	LaMnO$_3$ LaCoO$_3$	T$_{50}$: 301 °C T$_{50}$: 323 °C	-	-
	[61]	γ-MnO$_2$/SmMnO$_3$	T$_{50}$: 213 °C T$_{90}$: 226 °C	-	Toluene-Mn ions+ surface reactive oxygen → benzaldehyde → benzoic acid → chain carboxylic acids → CO$_2$.
	[62]	Mn/meso-TiO$_2$	-	-	Benzene → (splitting of benzene, hydrogenation, H abstraction by OH radicals) six-member ring cyclitols+aldehydes ketones etc. → a class of fulvene (isomerization) →CO$_2$ + H$_2$O.
	[63]	Mesoporous TiO$_2$	-	-	Benzene is mainly degraded by photo-generated electron–hole pairs and hydroxyl radicals.
	[64]	Graphite-SiO$_2$-TiO$_2$		The graphite-SiO$_2$-TiO$_2$ composites exhibited higher photocatalytic activity for degradation of benzene gas under visible light irradiation than that of pure TiO$_2$.	Optimum concentration of graphite facilitates the separation of photogenerated electron–hole pairs for graphite-SiO$_2$-TiO$_2$ composites by visible light.
	[65]	Pt/Al$_2$O$_3$	-	-	-

Table 4. *Cont.*

VOCs	Refer	Catalyst	Catalytic Performance	Remarks	Catalytic Mechanism
Toluene	[66]	2.3 wt% Pt/3DOM-Mn$_2$O$_3$	T$_{50}$: 165 °C T$_{90}$: 194 °C	-	A first-order reaction mechanism. Toluene → cat. Surface → benzyl alcohol → benzoic acid and benzaldehyde → (rise temperature) maleic anhydride → CO$_2$ and H$_2$O.
	[67]	Pd(shell)-Au(core)/TiO$_2$	T$_{50}$: 220 °C T$_{90}$: 230 °C	-	Langmuir-Hinshelwood mechanism.
	[68]	Au-Pd/CeO$_2$	T$_{50}$: 120 °C T$_{90}$: 150 °C	-	Due to the synergistic effect between Au and Pd nanoclusters, Au-Pd/CeO$_2$ bimetallic catalysts are much better than Au and Pd single metal catalysts.
	[69]	Mn$_2$O$_3$	T$_{50}$: 231 °C T$_{90}$: 239 °C	-	Toluene +cat. → benzyl species + active oxygen species → aromatic alkoxide → enzaldehyde → benzoate species+active oxygen specie → maleic anhydrides→CO$_2$.
	[58]	Layered copper manganese oxide (LCMO)	T$_{50}$: 187 °C T$_{90}$: 207 °C	-	-
	[59]	LaCoO$_3$	T$_{50}$: 244 °C	-	-
	[70]	La$_{0.8}$Sr$_{0.2}$CoO$_3$	T$_{50}$: < 160 °C T$_{99}$: 300 °C	-	Partial substitution of strontium (Sr) for lanthanum (La) greatly increased the oxygen vacancies in the surface regions to enhance catalytic activity.
	[71]	SrTi$_{1-X}$Cu$_X$O$_3$ SrTi$_{1-X}$Mn$_X$O$_3$	T$_{50}$: 343 °C T$_{90}$: 398 °C T$_{50}$: 302 °C T$_{90}$: 335 °C	-	Incorporation of Mn attributed a higher amount of oxygen vacancies in the perovskite surface to promote the toluene conversion. Supra facial mechanism.
	[72]	LaMn$_{1-x}$B$_x$O$_3$ (B = Co, Ni, Cu, Al)	T$_{50}$: 250 °C 234 °C 226 °C 242 °C T$_{90}$: none 278 °C 271 °C 318 °C	-	Addition of nickel into LaMnO$_3$ can improve the catalytic oxidation of toluene by the generation of more Mn^{4+} species and oxygen vacancies and the enhancing reducibility at a low temperature.

Table 4. *Cont.*

VOCs	Refer	Catalyst	Catalytic Performance	Remarks	Catalytic Mechanism
	[61]	γ-MnO2/SmMnO$_3$	T_{50}: 187 °C T_{90}: 208 °C	-	-
	[73]	LaMnO3/δ-MnO2	T_{90}: 258 °C	-	-
	[74]	LaMnO$_3$	T_{50}: 258 °C T_{90}: 275 °C	-	-
	[75]	MnO$_x$/H-Beta-SDS MnO$_x$/K-Beta-SDS MnOx/Si-Beta	T_{50}: 253, 262, 280 °C T_{90}: 285, 295, 312 °C	-	Mars-Van Krevelen mechanism. Organic molecules + lattice oxygen→oxygen vacancy + CO_2 + H_2O, oxygen vacancy + O_2→lattice oxygen.
	[76]	Mn/R-SBA-15	T_{98}: 240 °C	-	MVK mechanism. Mn_2O_3-MnO_2/R-SBA-15 supply more lattice oxygen species.
	[77]	LaFeO$_3$/black-TiO$_2$	The removal efficiency of black TiO$_2$ and LaFeO$_3$ for toluene was 89% and 98%, respectively, and the removal efficiency for IPA was 90% and 94%, respectively.	-	Cat.+photon (the wavelength shorter than 440 nm)→ electrons + O_2 →O^{2-}, O^{2-}+toluene and IPA → CO_2 + $H_2O_{(g)}$.
	[78]	Pd/CeO$_2$/γ-Al$_2$O$_3$	T_{98}: 205 °C	-	-
	[79]	CuO/ZnO Nanocomposite photocatalysts	-	-	Photooxidative activity and stability over ZnO are improved by loading CuO.
	[80]	FeO$_x$/SBA-15	-	Under the condition of 3% Fe loading, the oxidation of toluene is the best one.	(1) Direct removal caused by the collision of electrons or oxidation caused by the gas-phase radicals (O•, OH•, N$_2$•, NO•, NO$_2$•) in gas phase; (2) the reaction between adsorbed toluene or other intermediates and the active species (O•, OH•) on the catalyst surface. O_2 might be fixed on the catalyst surface via facile interconversion between Fe^{2+} and Fe^{3+} states and then be transported to the toluene or intermediates leading to CO_2 formation.

Table 4. *Cont.*

VOCs	Refer	Catalyst	Catalytic Performance	Remarks	Catalytic Mechanism
Butanol	[56]	0.3% Pt/γ-Al$_2$O$_3$	T$_{95}$: 200 °C	-	-
CH$_3$SSCH$_3$	[81]	Pt-Au/Ce-Al	T$_{50}$: 425 °C T$_{90}$: 480 °C	-	The addition of Au improved the selectivity of ceria-containing catalysts by decreasing the formation of byproducts. This may have had a connection to a lower amount of reactive oxygen after the Au addition.
	[81]	Cu-Au/Ce-Al	T$_{50}$: 275 °C T$_{90}$: 370 °C	–	-
Chlorobenzene	[82]	Pt/CrOOH	T$_{50}$: 340 °C T$_{90}$: 378 °C	-	Platinum accelerates the hydrolysis of Cr-Cl bonds formed at the CrOOH surface and determines the catalyst stability.
Dichloroethane	[82]	Pt/CrOOH	T$_{50}$: 283 °C T$_{90}$: 317 °C	-	-
Dichloromethane	[83]	CeO$_2$	T$_{90}$: 260 °C T$_{90}$: 160 °C	The addition of 3% (v/v) water can obviously inhibit the catalytic decomposition of VOCs on CeO$_2$.	Trichloroethylene + CeO$_2$ →C$_2$HCl→HCl, Cl$_2$, CO$_2$ and trace CO.
Dichlorobenzene	[84]	H-ZSM-5 and Na-ZSM-5	-	-	-
Trichloro benzene	[84]	H-ZSM-5 and Na-ZSM-5	-	-	-
DCE	[85]	CeO$_2$@SiO$_2$-400	T$_{50}$: 219 °C T$_{90}$: 275 °C	The conversion of 1 vol% H$_2$O and 3 vol% H$_2$O decreased by 6% and 19%, respectively.	DCE+acid sites→HCl+ VC. (1) VC→reactive carbonium ion→adsorbed alcohol species→acetate species. Or (2) VC→1,1,2-trichloroethane→dichloroethylene formed (subsequent chlorination reactions) →H$_2$O, CO$_x$ and HCl.
Ethylbenzene	[61]	γ-MnO$_2$/SmMnO$_3$	T$_{50}$: 201 °C T$_{90}$: 217 °C	-	-

Table 4. *Cont.*

VOCs	Refer	Catalyst	Catalytic Performance	Remarks	Catalytic Mechanism
Formaldehyde	[86]	TiO_2	TiO_2 degraded almost 100% of formaldehyde or acetaldehyde at a starting concentration of 400–500 ppb with a relative humidity of 40%.	-	The rate-determining step is the adsorption (external diffusion) on the catalysts active sites, thus the higher surface area, the higher the degradation.
Acetaldehyde	[86]	TiO_2	-	-	-
Acetone	[78]	$Pd/CeO_2/\gamma\text{-}Al_2O_3$	T_{98}:220 °C	-	-
	[87]	$CuO/g\text{-}Al_2O_3$	-	5.0 wt% $CuO/g\text{-}Al_2O_3$ catalyst has the highest removal rate of acetone, reaching 67.9%.	Both short-lived radicals and acetone/intermediates can be adsorbed on the catalyst surfaces to initiate a series of surface oxidation reactions, forming CO, CO_2, H_2O, and byproducts.
Ethyl acetate	[78]	$Pd/CeO_2/\gamma\text{-}Al_2O_3$	T_{98}:275 °C	-	-
Benzoquinone	[88]	$g\text{-}C_3N_4$	-	-	OH radicals+phenol→dihydroxycyclohexadienyl radical adducts→phenoxy radicals→H_2O(a very slow process), adducts+dissolved O_2→dihydroxy intermediates (-HO_2) →CO_2+H_2O.
Hydroquinone Catechol	[88]	$g\text{-}C_3N_4$	-	-	-

Table 4. *Cont.*

VOCs	Refer	Catalyst	Catalytic Performance	Remarks	Catalytic Mechanism
O-xylene	[89]	Ag/NiO$_x$-MnO$_2$	T$_{50}$: 145 °C T$_{90}$: 190 °C	The catalytic activity decreased with the addition of water vapor, but recovered after the removal of water vapor.	Mars-Van Krevelen mechanism. (i) Electrophilic O$_l$ +aromatic ring→maleate; (ii) O$_2$+ Cat.→electrophilic oxygen species (O$_2$$^{2-}$, O^{2-}, O$^-$), electrophilic oxygen species+aromatic ring→maleate, carbonate+(O$_2$. O$_2$$^{2-}$, O^{2-}, O$^-$ or O$_2$) +Ag→nucleophilic oxygen, nucleophilic oxygen + maleate and carboxylates→CO$_2$ and H$_2$O.
	[58]	Layered copper manganese oxide (LCMO)	T$_{50}$: 213 °C T$_{90}$: 227 °C	-	-
	[61]	γ-MnO2/SmMnO$_3$	T$_{50}$: 232 °C T$_{90}$: 250 °C	-	-
O-dichlorobenzene	[90]	CeMn30	GHSV = 15,000 mL/(g·h) T$_{50}$: 291 °C T$_{90}$: 347 °C GHSV= 7500 mL/(g·h) T$_{90}$: 224 °C GHSV = 30,000 mL/(g·h). T$_{90}$: 360 °C	The addition of low concentration of water vapor is beneficial to the early reaction, but will weaken the catalytic activity of catalyst.	O-dichlorobenzene molecules+basic oxygen (Mn-O-Ce-Vö, nucleophilic substitution)→HCl-H-O-Ce-Vö+phenyl. Mn-O-Ce weakened HCl-H-O-Ce-Vö and then prevented Deacon reaction and chlorine poisoning. Phenyl+ active lattice oxygen→organic intermediates →CO$_2$+H$_2$O. (Mars-Van Krevelen mechanism).
CO	[58]	Layered copper manganese oxide (LCMO)	T$_{50}$: 62 °C T$_{90}$: 76 °C	-	-
Cyclohexane	[70]	La$_{0.8}$Sr$_{0.2}$CoO$_3$	T$_{50}$: 180 °C T$_{99}$: 260 °C	-	-
CH$_3$SH	[91]	La(13)/HZSM-5	T$_{100}$: 40 °C	-	The La-modified HZSM-5 increased basic sites and displayed better adsorption ability to CH$_3$SH, decreased in strong acid sites and suppressed the formation of coke deposit.

Table 4. *Cont.*

VOCs	Refer	Catalyst	Catalytic Performance	Remarks	Catalytic Mechanism
C_2H_3CN	[92]	Cu-ZSM-5(SiO_2/Al_2O_3 = 26)	T_{90}: 325 °C	The catalyst has good resistance to steam poisoning.	Without H_2O: C_2H_3CN-SCC+O_2→NCO→oxidation products; with H_2O: C_2H_3CN-SCC+O_2 + H_2O→NH_3→products.
Cumene	[84]	H-ZSM-5 and Na-ZSM-5	-	-	-
Isopropanol	[60]	LaMnO$_3$ LaCoO$_3$	T_{50}: 216 °C 237 °C	-	-
	[79]	CuO/ZnO Nanocomposite photocatalysts	-	-	Photooxidative activity and stability over ZnO are improved by loading CuO.
	[93]	Au-Ag/CeO$_2$	T_{50}: 105 °C T_{90}: 158 °C	-	MVK redox mechanism.
Propyl alcohol	[60]	LaMnO$_3$ LaCoO$_3$	T_{50}: 203 °C 222 °C	-	-
	[70]	La$_{0.8}$Sr$_{0.2}$CoO$_3$	T_{90}: 160 °C	-	-
Propane	[94]	LaCoO$_3$	T_{50}: 208 °C T_{90}: 238 °C	-	MVK mechanism.
Methane	[95]	Nanocubic MnO$_2$	T_{50}: 293 °C T_{90}: 350 °C	-	CH_4+lattice oxygen or surface oxygen vacancies (MnO$_2$-C)→carboxylate species (Langmuir-Hinshelwood route), + active oxygen species→CO_2 and H_2O.

Table 4. *Cont.*

VOCs	Refer	Catalyst	Catalytic Performance	Remarks	Catalytic Mechanism
VOCs	[96]	MnO_2	T_{50}: 233 °C T_{90}: 256 °C	–	Toluene + Mn cations$\rightarrow CO_2$ and H_2O.
	[97]	$LaMnO_3$ and $LaCoO_3$	-	-	-
	[98]	La^{3+}-TiO_2 and Nd^{3+}-TiO_2	1.2% La^{3+}-TiO_2 had the highest photocatalytic activity.	-	-
	[99]	TiO_2/Pd	The conversion rate of VOCs reached 90% when the residence time was 27 s.	-	-
	[100]	$MesoTiO_2$/hydro-CF	-	-	Promotion effects on degradation of gaseous polar acetone come from well crystallized anatase nanocrystals, hydro-CF skeleton for adsorption, and fast mass transportation within the hierarchical frameworks.
	[101]	CsX, NaX, and HY	T_{100}: 200 °C	-	Mars-Van Krevelen mechanism, involving several redox steps.
O_3	[102]	Mn/ZSM-5	O_3 can be efficiently decomposed by the Mn/ZSM-5 and used for benzene degradation through the OZCO.	-	Benzene+•OH$\rightarrow$phenol$\rightarrow$benzoquinone$\rightarrow CO_2$ + H_2O.
	[103]	$CoMnO_x$/TiO_2	-	When the temperature is 320 °C, the decomposition efficiency of O_3 is 98%.	-
Vinyl chloride	[104]	HCl modified $La_{0.5}Sr_{0.5}MnO_3$	T_{100}: 300 °C	-	Doping and acid treatment obviously promote the active Mn^{4+} species amount and oxygen activation ability, and affect the chloric by-product distribution. Lower temperature inhibits the Deacon reaction and chlorination.

4.1. Catalytic Combustion

Catalytic combustion has received attention recently, as it shows great potential to address the shortcomings of the incineration method. Catalytic combustion is suitable for waste gas streams with low VOC concentrations and a moderate flow rate. Compared with the incineration method, catalytic combustion has been shown to efficiently remove VOCs from waste streams with a wide range of VOC concentrations. In addition, it operates at a lower temperature (293 versus 673 K) than incineration and resistant to the production of undesirable byproducts, such as dioxins and NO_x [105]. The diversity of VOC species necessitates the development of different kinds of catalysts for the combustion method, with commonly used catalysts including noble metals, non-noble metal oxides concentrated oxidation catalysts [1,2,41–44].

Previous reviews covering certain aspects of the catalytic combustion of VOCs have been published. For example, K. Everaert et al. reviewed, analyzed, and discussed the reaction kinetics, reactors, and reaction conditions of catalytic combustion research prior to 2004 [41]. Muhammad Shahzad Kamal et al. and Zhixiang Zhang et al. covered the recent progress in the development of combustion catalysts [2,44]. L.F. Liotta and W.B. Li et al. reviewed the mechanism of VOCs catalytic combustion over noble metal catalysts and non-noble metal catalysts, respectively [1,42]. In this section, we will briefly introduce the more recent development of new catalysts materials which have been used in this process, analyze the advantages and disadvantages they provide, and strategies for their successful implementation.

4.1.1. Noble Metal Catalysts

The general consensus of previous studies is that noble metal catalysts show the best catalytic performance in the combustion of non-halogenated VOCs. The noble catalysts which have been investigated include platinum, palladium, ruthenium, iridium, gold, and silver (Table 5) [2,41–44]. Due to their size-dependence catalytic properties and high price, noble metal catalysts are often supported on porous supports, such as γ-Al_2O_3, SiO_2, zeolite, and other non-metal oxides to increase the dispersion of noble metal nanoparticles and surface area, which can improve the catalytic efficiency of noble metal catalysts [106–111]. Catalysts are often supported on the substrate, which is in the form of a monolith or honeycomb material, such as cordierite, aluminum, and stainless steel [112]. Noble catalysts display high efficiencies for VOC removal at a lower temperature than other kinds of catalysts. Pt shows the best catalytic combustion of VOCs, exhibiting equal removal efficiencies at operating temperatures of up to 100 K lower than those used for other noble metals [42,44]. Two key factors were found to influence the catalytic performance of alumina supported Pt, dispersion and loading amount, with an increase in either of these properties associated with an obvious improvement of catalytic activity [106,113,114]. The metal particle size is also an important factor that influences the catalytic activity. Changes to the active metal particle size can also enhance catalytic performance. For instance, when the crystalline size of alumina supported Pt increased from 1.0 to 15.5 nm, the oxidation rate was found to increase by a factor of 10 [115]. The same phenomenon was also found in the oxidation of propylene over alumina supported Pt and Pd catalysts.

An important factor in the performance of noble metal catalysts for VOC combustion is specificity; in other words, the target VOCs molecules. For instance, P. Papaefthimiou et al. found that Pt and Pd supported on alumina showed good performance for the oxidation of benzene and butanol, but not ethyl acetate, with Pd generally outperforming Pt [57]. M. J. Patterson et al. discovered that alumina supported rhodium is the most active noble metal for 1-hexene, but not for aromatics, while benzene can be decomposed the most easily on platinum, and palladium showed the best catalytic performance in abatement of toluene [116]. The impact of certain non-VOC species in the waste stream can also impact performance, where these species can potentially 'poison' the catalyst or cause side reactions to occur. One example is the presence of CO, which was found to have little effect on the performance of Pd catalysts, but significantly inhibit the activity over Pt [117].

Table 5. Noble metal catalysts for catalytic combustion of VOCs.

Catalyst	VOCs	Catalytic Performance	Remarks	Catalytic Mechanism
0.3% Pt/γ-Al$_2$O$_3$	Butanol Benzene	T_{95}: 200 °C 220 °C	-	-
Pd-AuFeCeIM	Benzene	T_{100}: 200 °C	-	-
Pd(shell)-Au(core)/TiO$_2$	Toluene	T_{50}: 220 °C T_{90}: 230 °C	-	Langmuir-Hinshelwood mechanism.
Au-Pd/CeO$_2$	Toluene	T_{50}: 120 °C T_{90}: 150 °C	-	Due to the synergistic effect between Au and Pd nanoclusters, Au-Pd/CeO$_2$ bimetallic catalysts are much better than Au and Pd single metal catalysts.
Au-Ag/CeO$_2$	Isopropanol	T_{50}: 105 °C T_{90}: 158 °C	-	MVK redox mechanism.
Pt-Au/Ce-Al	CH$_3$SSCH$_3$	T_{50}: 425 °C T_{90}: 480 °C	-	The addition of Au improved the selectivity of ceria-containing catalysts by decreasing the formation of byproducts due to lower amount of reactive oxygen after the Au addition.
Cu-Au/Ce-Al	CH$_3$SSCH$_3$	T_{50}: 275 °C T_{90}: 370 °C	-	–
Ag/NiOx-MnO$_2$	O-xylene	T_{50}: 145 °C T_{90}: 190 °C	The catalytic activity decreased with the addition of water vapor, but recovered after the removal of water vapor.	Mars-Van Krevelen mechanism. (i) Electrophilic O$_l$ +aromatic ring→maleate; (ii) O$_2$+ Cat.→electrophilic oxygen species (O$_2^{2-}$, O^{2-}, O$^-$), electrophilic oxygen species + aromatic ring→maleate, carbonate+(O$_2$, O$_2^{2-}$, O^{2-}, O$^-$ or O$_2$) +Ag→nucleophilic oxygen, nucleophilic oxygen + maleate and carboxylates→CO$_2$ and H$_2$O.
2.3 wt% Pt/3DOM-Mn$_2$O$_3$	Toluene	T_{50}: 165 °C T_{90}: 194 °C	-	A first-order reaction mechanism. Toluene →cat. surface→benzyl alcohol→benzoic acid and benzaldehyde→(rise temperature) maleic anhydride→CO$_2$ and H$_2$O.

Transition metal oxides can be utilized as both supports and promoters for noble metal catalysts. Pt, Pd, Ru, Au supported on MgO, SnO_2, Co_3O_4, NiO, TiO_2, CeO_2, La_2O_3, ZrO_2 or PrO_2 have been explored for the oxidation of toluene, benzene, xylene, propene, light alkane, ethanol, propanol, butanol, formaldehyde, acetone, and acetic acid, respectively [42]. The role of the transition metal oxides is not only to supply a large surface area to disperse the noble metal particles, but in some cases, it can also improve the catalytic performance of noble metal particles by enhancing the mobility of lattice oxygen species. Previous studies showed that active oxygen species formed on cobalt oxide spinel-type crystallites can enhance the catalytic oxidation over PdO supported on alumina [118,119].

The reduction properties also influence the oxidation ability of supported noble metal catalysts. T. Mitsui et al. prepared SnO_2, CeO_2, and ZrO_2 supported Pt and Pd catalysts for the abatement of acetaldehyde [120]. These prepared catalysts were treated in an H_2/N_2 flow and calcined in the atmosphere. The results showed that the SnO_2 supported Pt and Pd showed the best catalytic performance among the calcined catalysts in the atmosphere, while after treatment in an H_2/N_2 flow, the catalytic activity of SnO_2 supported Pt and Pd decreased due to the formation of inactive inter-metallic phases (PtSn and Pd_3Sn_2). In contrast, CeO_2 and ZrO_2 supported catalysts showed the improved catalytic activity after reduction. In the elimination of formaldehyde over a TiO_2-supported catalyst, Pt/TiO_2 showed a superior catalytic performance to Rh/TiO_2, Pd/TiO_2, Au/TiO_2, and neat TiO_2 [121]. Other research showed that a series of supported Pt, Pd, and Au catalysts can even partially eliminate formaldehyde at room temperature [122].

Recently, the use of MnO_x based materials as catalyst supports has gained attention. In one instance, supporting Ag on NiO-doped MnO_2 showed a high activity towards the combustion of o-xylene [89]. The improvement in xylene oxidation was attributed to the enhanced oxygen activation and mobility afforded to the catalyst support via the addition of NiO and Ag. Wenbo Pei et al. explored the use of ordered, mesoporous Mn_2O_3 supports with embedded Pt particles for the catalytic combustion of toluene [66]. They found that the strong interaction between Pt and Mn_2O_3 in the ordered structure improves the activity and stability of the catalyst.

The single noble metal catalysts cannot satisfy the requirements of VOCs combustion. Therefore, some mixed noble metal catalysts have been developed to combine the advantages of different noble metal catalysts, such as Pt-Au, Cu-Au, and Pd-Au. T. Tabakova et al. found that the Pd deposition on the deposited gold showed the best catalytic performance for benzene combustion, which was totally eliminated at 200 °C. It also showed good stability [57]. M. Hosseini et al. showed that the deposition of palladium on aurum supported on TiO_2 (Pd(shell)-Au(core)/TiO_2) can significantly improve the catalytic activity for oxidation of toluene and propylene [67]. Der Shing Lee et al. deposited Au-Pd bimetallic nanoparticles on CeO_2 for toluene degradation, which showed a much better catalytic performance than Au/CeO_2 and Pd/CeO_2 catalysts due to the synergistic effect of gold and palladium [68]. The addition of non-noble metals also can improve the catalytic activity of noble metal catalysts. Roberto Fiorenza et al. prepared $Au-Ag/CeO_2$ and $Au-Cu/CeO_2$ bimetallic catalysts for alcohol oxidation and CO oxidation. These two catalysts showed higher selectivity for intermediate products higher CO conversion at a low temperature (100 °C) than Au/CeO_2 [93]. The addition of Au also can improve the performance of Al_2O_3 supported Cu-Pt catalysts in DMDS oxidation [81].

Noble metal catalysts showed a high catalytic activity and remarkable thermal stability in catalytic elimination of VOCs. However, the use of noble metal catalysts is also associated with distinct disadvantages. Firstly, the high cost of noble metal limits their application in the industrial abatement of VOCs. Secondly, the presence of chlorine, sulfur, CO, and water can suppress the catalytic performance significantly [42,123–125]. The regeneration and recycling of noble metal catalysts poisoned by Cl and S is difficult, so they are not suited to the treatment chlorine and sulfur-containing VOCs. In fact, the release of chlorine and sulfur containing VOCs is particularly common in pharmaceutical production processes, so chlorine- and sulfur-containing VOCs need to be removed prior to the treatment by noble metal catalysts, which will further increase the cost of waste gas purification.

4.1.2. Non-Noble Metal Catalysts

To address the cost of noble metals, non-noble metal oxides catalysts were developed for the abatement of VOCs. The materials which have been studied as non-noble metals include the derivatives of transition metals and rare earth elements, such as Ti, Cu, Mn, Al, Ce, Co, Fe, Cr, and V (Table 6) [1,126–129]. Although transition metal oxides catalysts generally showed a lower catalytic activity than noble metal catalysts for the oxidation of VOCs, they have many advantages, such as a resistance to chlorine and sulfur poisoning, tunable material properties, low cost, long on-stream lifetime, easy regeneration, and low environmental impact. The non-noble metal oxides catalysts applied and studied in VOCs abatement include CuO_x, MnO_2, FeO_x, NiO_x, CrO_x, and CoO_x.

The non-noble metal oxides catalyst systems which we will discuss include ones in which the metal oxide is both supported or unsupported. Due to the presence of mobile oxide species in lattice, Co_2O_3 displays excellent reduction and oxidation abilities. As such, studies have shown Co_2O_3 to be one of the best catalysts used for the combustion of benzene, toluene, propane, 1,2-dichloroethane, and 1,2-dichlorobenzene [130–133]. The catalytic activity of Co_2O_3 is determined by the method of preparation, treatment conditions, and surface area.

MnO_2 is another commonly used metal oxide catalyst, which has been applied and studied in the abatement of n-hexane, acetone, benzene, ethanol, toluene, propane, trichloroethene, ethyl acetate, and NO_x [133–139]. The catalytic activity can be tuned by the preparation method and depends on the structure, surface area, support materials, and oxidation states of catalysts. In the catalytic combustion of ethyl acetate and hexane, MnO_2 even achieved a better activity than Pt/TiO_2 [140]. Yonghui Wei et al. removed the La atoms from the $LaMnO_3$ perovskite to prepare MnO_2 with a high surface area (>150 m^2/g), upon which it showed excellent catalytic activity in the oxidation of toluene [96]. Zhang Kai et al. synthesized the nano-cubic MnO_x which has a large specific surface area, many oxygen vacancies, and good low temperature reducibility. The conversion of toluene via combustion was more than 90% at 350 °C [95]. Xueqin Yang et al. found that the acid treatment did not change the morphology of the catalyst, but could improve the oxidation ability of the catalyst by increasing the number of Mn^{4+} species and structural defects on the surface of the catalyst [69]. A common theme throughout the implementation of Mn-based metal oxide catalysts for VOC oxidation is the availability and mobility of oxygen within the MnO_x, which is attributed to the oxidation and reduction ability of the Mn afforded by the multiple oxidation states in which it can exist.

Copper oxides are another kind of efficient catalysts used in total oxidation of methane, methanol, ethanol, and acetaldehyde [141,142]. The main factors which influence the catalytic activity are the Cu oxidation state and the availability of lattice oxygen. The addition of other metal oxides, such as CeO_2, can enhance the catalytic ability noticeably [133].

Chromium oxides are also promising oxidation catalysts, especially for the combustion of halogenated VOCs [124,133,143]. For chromium oxides, highly crystalline samples showed a better catalytic activity than amorphous ones [144]. Rotter et al.'s research showed that, when using TiO_2 as a support material, chromium oxides achieved higher catalytic oxidation of trichloroethylene than manganese oxide, cobalt oxide, and iron oxide [82]. Chromium has also been successfully supported on silica, alumina, porous carbon, and clay to eliminate pollutants such as carbon tetrachloride, chloromethane, trichloroethylene, ethyl chloride, chlorobenzene, and perchloroethylene [142]. However, chromium oxides also suffer deactivation due to the reaction between chromium and chlorine to form Cr_2Cl_2 [145,146].

CeO_2 is a widely used catalyst in oxidation reactions due to its strong interactions with other metals, high oxygen storage capacity, and ready shuttling between the Ce^{3+} and Ce^{4+} states [147–149]. Dai et al. compared the removal of chlorinated alkanes and alkylenes over CeO_2 [83]. The results showed that CeO_2 is more efficient when it comes to oxidizing chlorinated alkanes than chlorinated alkylenes. CeO_2 also faced the deactivation problem due to the absorption of Cl_2 and HCl on the surface [150], so the design of chlorine resistance metal oxide catalysts is still a challenge which must be overcome.

Vanadium oxides were also developed to decompose chlorinated VOCs, such as polychlorinated pollutants and dichlorobenzene due to its tolerance of chlorine and sulfur compounds [151]. The presence of water can enhance and suppress the catalytic activity of V_2O_5 via the removal of surface absorbed chlorine and reduction of active sites, respectively [152]. Other non-noble metal oxides were also investigated for abatement of VOCs, such as NiO and FeO_x, which require further improvement of catalytic efficiency [153].

The above discussion suggests that the use of a single metal oxide as VOC oxidation catalysts is too often plagued by either a low catalytic activity or catalyst poisoning. Thus, focus has shifted to the development of mixed metal oxide catalysts such as Mn-Ce, Mn-Cu, Co-Ce, Sn-Ce, Mn-Co, and Ce-Cu oxides [119,154–157]. The logic here is that combining two metal oxides with different materials and catalytic properties allows for a synergistic enhancement in performance. The previous studies showed that the rate determining step of VOC catalytic combustion was the oxygen removal from the catalysts lattice [119], so the goal of mix-metal oxides catalysts design was the enhancement of the lattice oxygen species availability.

The addition of copper into CeO_2 can promote the catalytic efficiency due to a synergistic effect, leading to a highly efficient decomposition of ethyl acetate, ethanol, propane, benzene, and toluene [158–160]. MnO_x-CeO_2 has been applied for the destruction of ethanol, formaldehyde, hexane, phenol, ethyl acetate, and toluene [155,161–164]. Mn-Co oxides catalysts also showed improved catalytic activity relative to either MnO_x or Co_2O_3 in the combustion of ethyl acetate and n-hexane [100]. CeO_2-CrO_x showed excellent catalytic activity for the decomposition of chlorinated VOCs [165], while the removal of chlorobenzene over MnO_x-TiO_2 and MnO_x-TiO_2-SnO_x showed much better catalytic performance than not only the individual oxides, but also achieved removal efficiencies on par with noble metal catalysts [166]. A three-dimensional ordered mesoporous material of mixed cerium-manganese oxide was prepared for the efficient catalytic combustion of chlorine-containing VOCs due to its large specific surface, enriched Ce^{3+} content, oxygen vacancies, active oxygen species, and acidic sites. It showed good water resistance and high airspeed applicability. However, catalyst deactivation caused by inorganic chlorine adsorption still occurred [90]. Layered copper manganese oxide has been prepared for the catalytic combustion of CO and VOCs, which showed efficient activity due to the interfacial structure of mixed phases and the formation of the Cu^{2+}-O^{2-}-Mn^{4+} entity [58]. Acidic sites can be provided by support to prevent the decrease of catalytic activity. CeO_2@SiO_2 was prepared to catalyze the combustion of 1,2-dichloroethane. SiO_2 can provide weak acid sites, as well as promote the adsorption and activation of 1,2-dichloroethane and the desorption of generated HCl [85].

A vast number of preparation methods exist for the synthesis of mixed metal oxide catalysts, including thermal decomposition, impregnation, co-precipitation, and the sol-gel method [167–169]. The selection of preparation methods depends on the properties of catalysts and the application situation. Furthermore, as discussed above, complex ordered microporous, multilayer or core-shell structures have recently been applied to catalytic oxidation processes to access properties which come from having a highly controlled particle composition and morphology. The chance to alter not only the metal centers present within mixed metal oxide systems, but also the relative metal ratios.

Table 6. Non-noble metal catalysts for catalytic combustion of VOCs.

Refer	Catalyst	VOCs	Catalytic Performance	Remarks
[69]	Mn_2O_3	Toluene	T_{50}: 231 °C T_{90}: 239 °C	-
[82]	Pt/CrOOH	Dichloroethane	T_{50}: 283 °C T_{90}: 317 °C	-
		Chlorobenzene	T_{50}: 340 °C T_{90}: 378 °C	
[83]	CeO_2	Tetrachloroethylene dichloromethane	T_{90}: 260 °C T_{90}: 160 °C	The addition of 3% (v/v) water can obviously inhibit the catalytic decomposition of VOCs on CeO_2.
[90]	CeMn30	O-dichlorobenzene	GHSV = 15,000 mL/(g·h) T_{50}: 291 °C T_{90}: 347 °C GHSV= 7500 mL/(g·h) T_{90}: 224 °C GHSV = 30,000 mL/(g·h) T_{90}: 360 °C	The addition of low concentration of water vapor is beneficial to the early reaction, but will weaken the catalytic activity of the catalyst.
[96]	MnO_2	VOCs	T_{50}: 233 °C T_{90}: 256 °C	-
[95]	Nanocubic MnO_2	Methane	T_{50}: 293 °C T_{90}: 350 °C	-

4.1.3. Perovskite Catalysts

Perovskite-type oxides are a kind of composite oxides which have a similar structure with $CaTiO_3$, and can be expressed by ABO_3. The common way to modify the perovskite catalysts is replacement of the cation B by B' to tune the redox ability or enhance the stability [1]. With the replacement of the cation B, the crystal lattice would be distortion which leads to the enhancement of redox ability and improvement of stability. The most commonly used perovskite for catalytic combustion of VOCs is $LaBO_3$, in which B can be Co, Fe, Ni, Mn, and Sr (Table 7) [60,97,170,171]. Huang et al. used Sr partially replaced La in $LaCoO_3$ for catalytic combustion of propyl alcohol, toluene, and cyclohexane [70]. The results showed that the doped $LaCoO_3$ showed a better catalytic performance than the undoped one, and the modified catalysts were stable in the reaction. R. Spinicci et al. compared the catalytic activity of $LaMnO_3$ and $LaCoO_3$ for catalytic combustion of acetone, isopropanol, and benzene [60]. They suggested that $LaMnO_3$ showed a better performance than $LaCoO_3$. In oxidation of isopropanol, acetone was the intermediate product. The surface oxygen species played a key role in this process. The increase of oxygen pressure is positive for the catalytic combustion of VOCs over these perovskite catalysts. G. Sinquin et al. applied $LaMnO_3$ and $LaCoO_3$ for the catalytic combustion of chlorinated VOCs, such as CH_2Cl_2 and CCl_4. $LaMnO_3$ showed a better chlorine resistance than $LaCoO_3$ [97]. Mihai Alifanti et al. supported $LaCoO_3$ on cerium-zirconium oxides ($Ce_{1-x}Zr_xO_2$, x = 0–0.3) for the catalytic combustion of benzene and toluene [172]. The results showed that all the supported catalysts showed a better performance than $Ce_{1-x}Zr_xO_2$ and 20% loaded $LaCoO_3$ showed about 10 times higher catalytic activity than $LaCoO_3$ for toluene oxidation due to its large surface area and good oxygen mobility. S. I. Suárez-Vázquez et al. synthesized $SrTi_{1-x}B_xO_3$ (B = Mn, Cu) for toluene destruction [71]. Mn could replace Ti and enter the perovskite structure, while Cu could not. The Mn doped catalysts showed the highest catalytic activity and can completely decompose toluene to CO_2 at a temperature lower than 350 °C. Perovskite also can be prepared from solid waste such as the obsoleting lithium battery. Mingming Guo et al. prepared manganese-based perovskite catalyst from the waste lithium battery for catalytic combustion of toluene, which showed a better catalytic activity than pure manganese perovskite catalyst due to more Mn^{4+} ions and lattice oxygen species, as well as high specific surface area [72]. In order to increase the amounts of active sites, Junxuan Yao et al. removed the La ions from $LaCoO_3$ to obtain the disordered Co_3O_4. It showed a better catalytic activity for propane combustion than the one prepared by other methods [94]. To further improve the catalytic activity, γ-MnO_2 was calcined on the surface of $SmMnO_3$ which had a large specific surface area, high Mn^{4+}/Mn^{3+} and O_{latt}/O_{ads}. Compared with $SmMnO_3$, it showed a better catalytic activity and stability (10 vol% water) in the process of catalytic reaction [61]. Jingsi Yang et al. assembled the $LaMnO_3$ perovskite in MnO_2 and adjusted La/Mn to 15. The redox ability of the catalyst was improved by enhancing the interaction between the active phase and the support [73]. The ratio of citric acid and metal ion ($La^{3+}Mn^{2+}$) was also tested to find out the best composite of perovskite catalysts. Zakaria Sihaib et al. prepared $LaMnO_3$ with different ratios. The results show that the catalyst with the ratio of 0.5 to 1.5 has the best catalytic performance and the amount of citric acid affects the specific surface area of perovskite catalyst [74]. Li Wang et al. added Sr into the $LaMnO_3$ to prepare $La_{0.5}Sr_{0.5}MnO_3$. The amount of Mn^{4+} and the oxidation ability of vinyl chloride has been improved after HCl modification [104]. The perovskite catalysts showed a good catalytic activity for combustion of VOCs at low temperature due to their tunable redox property by replacing the B atom. However, they also have some disadvantages, such as low thermal stability. The catalytic activity and stability of perovskite catalysts need to be further improved.

Table 7. Perovskite catalysts for catalytic combustion of VOCs.

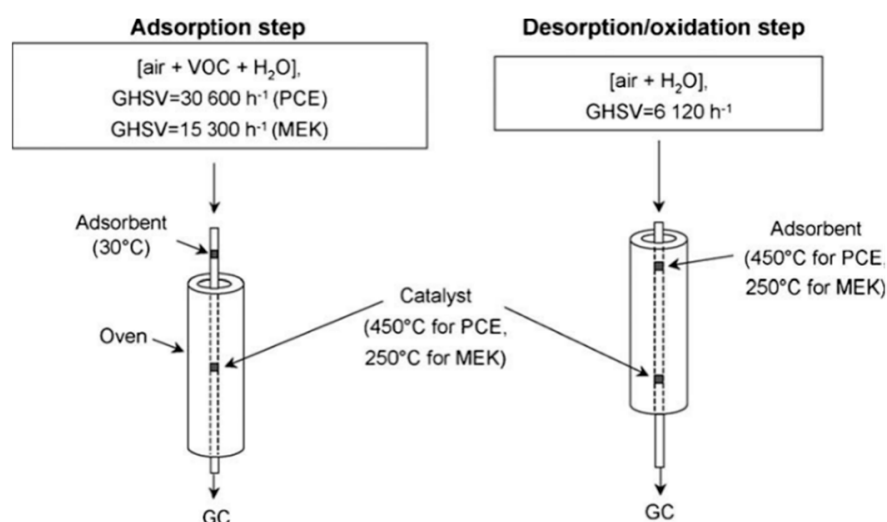| Refer	Catalyst	VOCs	Catalytic Performance	Remarks	Catalytic Mechanism
[58]	Layered copper manganese oxide (LCMO)	CO Benzene Toluene O-xylene	T_{50}: 62 °C T_{90}: 76 °C T_{50}: 218 °C T_{90}: 240 °C T_{50}: 187 °C T_{90}: 207 °C T_{50}: 213 °C T_{90}: 227 °C	The introduction of water vapor had no significant effect on the catalyst. The catalyst activity decreased about 30% after SO_2 was added. The addition of CO_2 has no effect on the catalytic activity of the catalyst.	The larger surface area and the formation of Cu^{2+}-O^{2-}-Mn^{4+} entities at the interface between CuO and layered MnO_2 promoted the CO and VOCs oxidation.
[59]	LaCoO$_3$	Benzene Toluene	T_{50}: 330 °C T_{50}: 244 °C	Water vapor has no significant effect on the catalytic performance of catalyst.	Factors improve activity: (i) The larger exposed surface, (ii) the composition of the support provides increased oxygen mobility.
[60]	LaMnO$_3$ LaCoO$_3$	Isopropanol Benzene Propyl alcohol Isopropanol Benzene Propyl alcohol	T_{50}: 216 °C 301 °C 203 °C T_{90}: 237 °C 323 °C 222 °C	-	-
[61]	γ-MnO2/SmMnO$_3$	Toluene Benzene O-xylene Ethylbenzene	T_{50}: 187 °C T_{90}: 208 °C T_{50}: 213 °C T_{90}: 226 °C T_{50}: 232 °C T_{90}: 250 °C T_{50}: 201 °C T_{90}: 217 °C	-	Toluene-Mn ions+ surface reactive oxygen → benzaldehyde → benzoic acid → chain carboxylic acids → CO_2.

Table 7. *Cont.*

Refer	Catalyst	VOCs	Catalytic Performance	Remarks	Catalytic Mechanism
[70]	$La_{0.8}Sr_{0.2}CoO_3$	toluene Cyclohexane Propyl alcohol	T_{50}:<160 °C T_{99}: 300 °C T_{50}: 180 °C T_{99}: 260 °C T_{90}: 160 °C	-	Partial substitution of strontium (Sr) for lanthanum (La) greatly increased the oxygen vacancies in the surface regions to enhance the catalytic activity.
[71]	$SrTi_{1-X}Cu_XO_3$ $SrTi_{1-X}Mn_XO_3$	Toluene	T_{50}: 343 °C T_{90}: 398 °C T_{50}: 302 °C T_{90}: 335 °C	-	Incorporation of Mn attributed a higher amount of oxygen vacancies in the perovskite surface to promote the toluene conversion. Supra facial mechanism.
[72]	$LaMn_{1-x}B_xO_3$ (B = Co, Ni, Cu, Al)	Toluene LMLi LMNi LMCo LMAl LMLi LMNi LMCo LMAl	T_{50}: 250 °C 234 °C 226 °C 242 °C T_{90}: none 278 °C 271 °C 318 °C	-	Addition of nickel into $LaMnO_3$ can improve the catalytic oxidation of toluene by generation of more Mn^{4+} species and oxygen vacancies and the enhancing reducibility at low temperature.
[73]	LaMnO3/δ-MnO2	Toluene	T_{90}: 258 °C	-	-

Table 7. *Cont.*

Refer	Catalyst	VOCs	Catalytic Performance	Remarks	Catalytic Mechanism
[74]	LaMnO$_3$	Toluene	T$_{50}$: 258 °C T$_{90}$: 275 °C	-	-
[85]	CeO$_2$@SiO$_2$-400	DCE	T$_{50}$: 219 °C T$_{90}$: 275 °C	The conversion of 1 vol% H$_2$O and 3 vol% H$_2$O decreased by 6% and 19%, respectively.	DCE+acid sites→HCl+ VC. (1) VC→reactive carbonium ion→adsorbed alcohol species→acetate species. Or (2) VC→1,1,2-trichloroethane→ dichloroethylene formed (subsequent chlorination reactions) →H$_2$O, CO$_x$ and HCl.
[94]	LaCoO$_3$	Propane	T$_{50}$: 208 °C T$_{90}$: 238 °C	-	MVK mechanism.
[97]	LaMnO$_3$ and LaCoO$_3$	Chlorinated VOCs	-	-	-
[104]	HCl modified La$_{0.5}$Sr$_{0.5}$MnO$_3$	Vinyl chloride	T$_{100}$: 300 °C	-	Doping and acid treatment obviously promote the active Mn^{4+} species amount and oxygen activation ability, and affect the chloric byproduct distribution. The lower temperature inhibits the Deacon reaction and chlorination.

4.1.4. Concentrated Oxidation Catalysts

The low concentration of VOCs can limit the catalytic efficiency of catalysts. Some porous materials were investigated to the concentration and decomposition of VOCs, such as zeolite, γ-Al$_2$O$_3$ (Table 8, Figure 13) [84,101,173–175]. R. Beauchet et al. tried to decompose the isopropanol and o-xylene mixture over the CsX, NaX, and HY zeolite [173]. O-xylene and isopropanol were totally decomposed at 250 °C over the NaX zeolite. The addition of Pt on the zeolite can significantly increase the catalytic activity. The main obstacle for the application of zeolite was the coke that formed during the reaction, which led to the short lifetime. Amir Ikhlaq et al. studied the mechanism and kinetics of decomposition of chlorinated VOCs by ozonation over the γ-Al$_2$O$_3$ and ZSM-5 zeolite [174]. The results suggest that ozone reacts with the absorbed VOCs on the surface of catalysts. However, the ozonation process will increase the cost in most of the industrial processes. Yuexin Peng et al. supported MnO$_2$ on the Al-rich β-zeolite to degrade toluene [75]. The T$_{90}$ is 285 °C, which is much lower than the MnO$_2$ supported on γ-Al$_2$O$_3$ due to the lattice oxygen species in MnO$_2$ and absorbed oxygen species on the zeolite. Cu and Co were also used to modify the β-zeolite for the destruction of toluene and trichloroethylene [76]. The modified zeolite showed good stability in the reaction. The catalytic activity is mainly from the supported metal oxides. The suitable acidity and strong oxidation stability can improve the CO$_2$ selectivity. Dedong He et al. modified the HZSM-5 zeolite with a series of rare earth elements, including La, Ce, Pr, Nd, Sm, Y, and Er, for the catalytic decomposition of CH$_3$SH [91]. Cu was also used to modify ZSM-5 for the combustion of acrylonitrile. The isolated Cu is the active center. The SiO$_2$/Al$_2$O$_3$ ratio can affect the ion exchange capacity and the catalytic performance of the catalyst. When the ratio is 26, the catalyst shows the best catalytic activity [92]. SBA-15 was used to support MnO$_x$ for the combustion of toluene and showed good catalytic activity [176]. The La modified HZSM-5 zeolite showed much better activity and stability than HZSM-5 due to the tunable acidity, which can promote the adsorption and activation of the CH$_3$SH molecule and inhibit the formation of coke deposit. The previous researches showed the potential application in the industry. However, to fulfill the requirements of the industry, the concentration-catalysis process to remove VOCs needs more research on lifetime, catalytic efficiency.

Figure 13. Scheme of adsorption/oxidation apparatus. Reprinted with permission from [1], 2009, Elsevier Ltd.

Table 8. Concentrated oxidation catalysts for catalytic combustion of VOCs.

Refer	Catalyst	VOCs	Catalytic Performance	Remarks	Catalytic Mechanism
[75]	MnO$_x$/H-Beta-SDS MnO$_x$/K-Beta-SDS MnOx/Si-Beta	Toluene	T$_{50}$: 253, 262, 280 °C T$_{90}$: 285, 295, 312 °C	-	Mars-Van Krevelen mechanism. Organic molecules+lattice oxygen→oxygen vacancy+CO$_2$+H$_2$O, oxygen vacancy+O$_2$→lattice oxygen.
[84]	H-ZSM-5 and Na-ZSM-5	Cumene Dichlorobenzene Trichloro benzene	-	-	-
[91]	La(13)/HZSM-5	CH$_3$SH	T$_{100}$: 40 °C	-	The La-modified HZSM-5 increased basic sites and displayed better adsorption ability to CH$_3$SH, decreased in strong acid sites and suppressed the formation of coke deposit.
[92]	Cu-ZSM-5(SiO$_2$/Al$_2$O$_3$ = 26)	C$_2$H$_3$CN	T$_{90}$: 325 °C	The catalyst has good resistance to steam poisoning.	Without H$_2$O: C$_2$H$_3$CN-SCC+O$_2$→NCO→oxidation products; with H$_2$O: C$_2$H$_3$CN-SCC+O$_2$+ H$_2$O→NH$_3$→products.
[101]	CsX, NaX, and HY	VOCs mixture	T$_{100}$: 200 °C	-	Mars-Van Krevelen mechanism, involving several redox steps.
[176]	Mn/R-SBA-15	Toluene	T$_{98}$: 240 °C	-	MVK mechanism. Mn$_2$O$_3$-MnO$_2$/R-SBA-15 supply more lattice oxygen species.

4.1.5. The Influence Factors on Catalytic Performance

In the real industrial process, a lot of factors influence the catalytic efficiency. Firstly, the kind of VOCs determines the selection of catalysts. For example, noble metal catalysts show the best VOCs eliminating efficiency, but they are not suitable for the destruction of chlorine and sulfur containing VOCs due to the poison of the catalysts. Secondly, the surface area of the catalysts is the main factor that influences the catalytic activity. Research shows that MnO_2 with a higher surface area showed much better catalytic performance than the one with a lower surface area [133]. Thirdly, the crystal type of catalysts also influences the catalytic performance of the catalysts with the same content. For instance, the catalytic performance of TiO_2 with different crystal types, namely rutile and anatase, showed a different catalytic activity [121,167]. The humidity is the common content in the industrial waste gas. In most of the reports, water molecules can suppress the catalytic activity due to the complete adsorption on active sites and destruction of catalysts [177]. In other researches, humidity plays a positive role in the oxidation. In the catalytic combustion of chlorobenzene over VO_x/TiO_2, VO_x-WO_x/TiO_2, and VO_x-MoO_x/TiO_2, water can remove the adsorbed Cl^- from the catalysts surface and react with chlorine to produce HCl [134]. The water vapor can show a different effect on the same VOCs over different catalysts. Kullavanijayam et al. reported that water enhanced the catalytic oxidation of cyclohexene over the ceria–alumina supported Pt and Rh, but it had a negative effect on the oxidation of cyclohexane over the ceria–alumina supported Pd catalyst [178]. CO is another poison for precious metal catalysts, so during the catalytic combustion, enough air is needed to avoid the generation of CO. The life of catalysts is also important for catalytic combustion. The main obstacle for the development of catalysts for the catalytic combustion of halogen and sulfur containing VOCs is the short life of common catalysts. Although V oxides show less catalytic efficiency than other catalysts, it is still used in the elimination of halogen and sulfur containing VOCs due to its long catalytic life [152]. Since after the installation of catalytic combustion equipment, it will be in operation for a long time, therefore, the life of the catalysts determines the cost of catalytic combustion.

The catalytic combustion process has been well developed in recent years. The diversity of the catalysts has been investigated. However, there are still some obstacles on the way to the industrial application, such as short lifetime, high cost, and no universality to different kinds of VOCs. More work should be done on these problems.
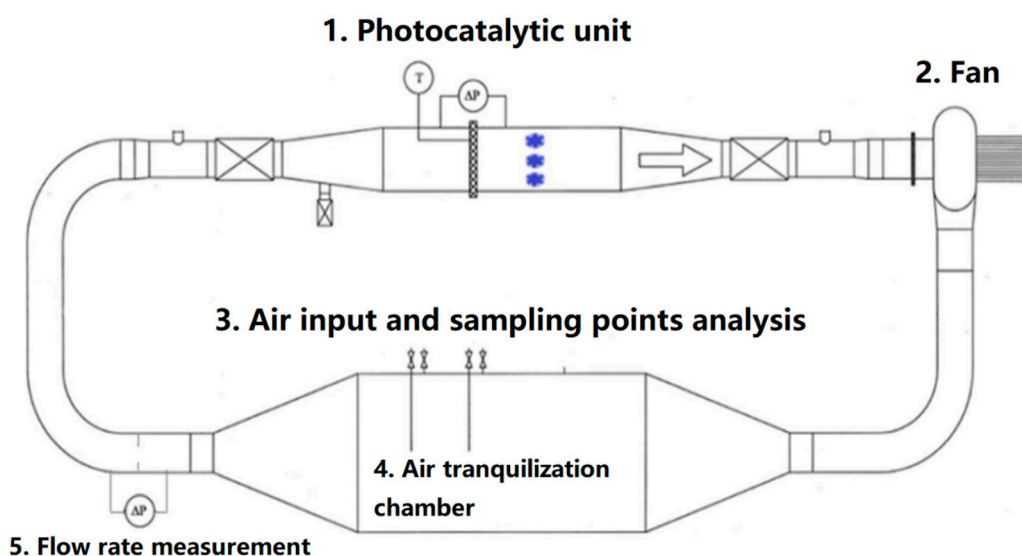
4.2. Photocatalytic Oxidation

Photocatalytic reactions have drawn a lot of attention and have been well developed in recent years since Fujishima found the splitting water to H_2 and O_2 over TiO_2 [55,179,180]. Different kinds of photocatalysts have been developed to treat VOCs containing waste water, such as TiO_2, WO_3, ZnO_2, CdS, g-C_3N_4, and BiOBr (Table 9) [56,180–185]. The mechanism of photocatalysis is that when the light with a suitable wavelength radio on catalysts (semiconductors), the electrons and holes were separated and generated on the surface of catalysts, then the radicals of •OH and O^{2-} was formed on the surface of catalysts, the VOCs reacted with these radicals and decomposed to CO_2 and H_2O at last [186,187]. In the water solution, water can react with the catalysts and form •OH, which is positive for the decomposition of VOCs in water. The photocatalytic elimination of VOCs in the gas phase follows a similar mechanism, but the radicals are main O^{2-} due to the shortage of humidity. In this section, the progress in the elimination of VOCs in the gas phase by photocatalytic methods was mainly discussed.

The most studied photocatalyst for the elimination of VOCs is TiO_2 [44]. Wilson F. Jariam et al. degraded 17 kinds of VOCs with the concentration range of 400–600 ppmv over TiO_2 under the radiation of ultraviolet light [98]. The results showed that trichloroethylene (99.9%), isooctane (98.9%), acetone (98.5%), methanol (97.9%), methyl ethyl ketone (97.1%), t-butyl methyl ether (96.1%), dimethoxymethane (93.9%), methylene chloride (90.4%), methyl isopropyl ketone (88.5%), isopropanol (79.7%), chloroform (69.5%), and tetrachloroethylene (66.6%) were decomposed efficiently over TiO_2. The photodegradation of isopropylbenlene (30.3%), methyl chloroform (20.5%), and pyridine (15.8%)

on TiO_2 was not as efficient as other VOCs. The catalytic lifetime was also tested by toluene. The conversion of toluene decreased to 20.9% after a 150 min test, but the deactivated catalysts can be easily regenerated by washing with H_2O_2 and illumination. F. B. Li et al. prepared La ion doped TiO_2 by the sol-gel method for photodegradation of benzene, toluene, ethylbenzene, and o-xylene in the gas phase [188]. The results showed that the La ion doped TiO_2 performed much better than the pure TiO_2. This was due to the improved adsorption ability and the enhanced electron–hole pairs separation by the presence of Ti^{3+} and the electron transfer between the conduction band/defect level and lanthanide crystal field state. Tânia M. Fujimoto et al. supported the palladium on TiO_2 for the photocatalytic decomposition of octane, isooctane, n-hexane, and cyclohexane in a low concentration (100~120 ppmv) [99]. The modified catalysts showed excellent catalytic activity in the decomposition of VOCs rapidly. V. Héquet et al. used a closed-loop reactor to study the mixture effect over the P_{25} TiO_2/SiO_2 mixture (Figure 14) [189]. They have developed the accurate analytical methods to identify and quantify the majority of the potential formed intermediates, which provide an efficient way to study the reaction mechanism. Yajie Shu et al. used Mn doped TiO_2 to degrade benzene by O_3 under vacuum ultraviolet (VUV) irradiation [62]. The doped TiO_2 showed better performance than the undoped one and P_{25} due to the formation of highly reactive oxidizing species. Jian Ji et al. showed that compared with the one without UV radiation, the UV radiation can improve the removal efficiency of benzene by about 10% (Figure 15) [63]. Marta Stucchi et al. developed a simultaneous photodegradation system for the VOC mixture elimination by TiO_2 powders, which showed a good efficiency [86]. Huiling Huang et al. developed Mn modified ZSM-5 as catalysts for VUV photolysis combined with ozone-assisted catalytic oxidation and studied the mechanism [102]. The catalysts showed good efficiency. Although most of the catalysts showed excellent activity in the elimination of VOCs under UV light, the light utilization efficiency was still low due to the low percent of the UV light in nature light. Xufang Qian et al. designed mesoporous TiO_2 films coated with carbon foam for photodegradation of acetone and toluene, which can converse more than 90% of VOCs to CO_2 under visible light due to the plausible carbon doping and the strong interaction between the TiO_2 precursor and the hydro-carbon foams [100]. The graphite-SiO_2-TiO_2 composite and BiOBr@SiO_2 flower-like nanospheres were also used for photodegradation of VOCs under visible light and showed good catalytic activity [64]. The low solar utilization ratio was the main obstacle to improve photocatalytic efficiency. In order to improve the efficiency, materials with a good light adsorption ability was applied. Yun-En Lee et al. prepared black-TiO_2 and LFO/black-TiO_2 and they showed excellent photo catalytic activity for the removal of toluene and IPA due to their good light adsorption ability [77]. The modification of g-C_3N_4 by hydroxyl groups can enhance visible light-driven photocatalytic properties of g-C_3N_4 obviously which can improve the adsorption energy of g-C_3N_4 for water and phenol [88]. The structure of catalysts was also carefully tuned to improve the catalytic activity [190]. Bettini S et al. insulated a layer of SiO_2 between zinc oxide and nano silver and controlled the thickness of the insulated layer, which enhanced the photocatalytic oxidation ability of the catalyst significantly [78]. The photocatalytic activity of ZnO can also be improved by doping CuO [191]. The photocatalytic elimination of VOCs is one of the most promising methods. However, the industrial application of this method is still a problem.

1. Photocatalytic unit

2. Fan

3. Air input and sampling points analysis

4. Air tranquilization chamber

5. Flow rate measurement

Figure 14. A 420-L of continuous closed-loop photocatalytic reactor: (**1**) Photocatalytic unit containing the TiO$_2$ photocatalytic medium and the ultraviolet (UV) lamps, (**2**) fan, (**3**) air input and sampling points for analysis, (**4**) air tranquilization chamber, (**5**) flow rate measurement. Reprinted with permission from [176], 2018, Elsevier Ltd..

VUV-PCO system

Gas distributing system

Analysis system

Zero air generator

Humidometer

Water

Mass flow Benzene Buffer controller

UV lamps

Catalyst

Support ring

Valve　**To air**

GC

Ozone analyzer
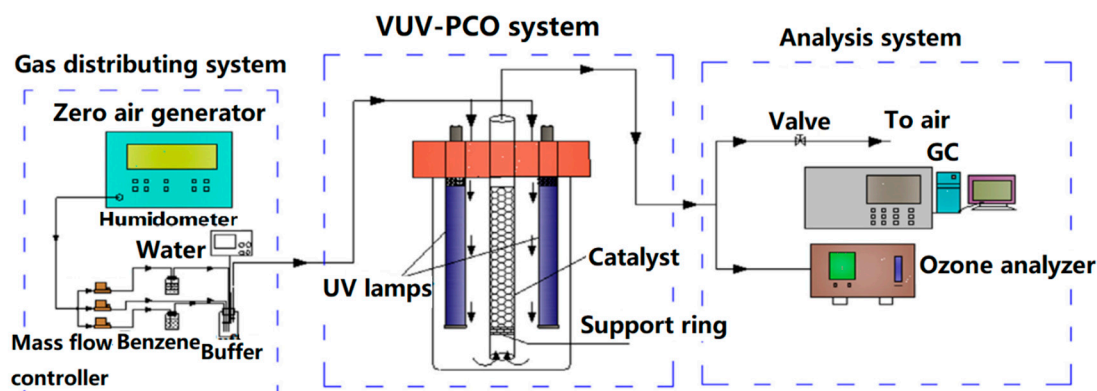
Figure 15. The schematic diagram of the VUV-PCO system. Reprinted with permission from [63], 2017, Elsevier Ltd.

There is a large amount of reports on the photocatalytic elimination of VOCs. The advantages of this process are green, energy saving, and clean. However, the reported catalysts are not efficient enough for an industrial application at the present stage. Firstly, the reaction needs more time than other methods. Secondly, most of the reported catalysts could not use visible light as energy to start the reactions, which limited the improvement of quantum efficiency, so it still needs to develop efficient photocatalysts and design effective reaction systems.

Table 9. Photocatalysts for elimination of VOCs.

| Refer	Catalyst	VOCs	Catalytic Performance	Remarks	Catalytic Mechanism
[62]	Mn/meso-TiO_2	Benzene	-	-	Benzene→(splitting of benzene, hydrogenation, H abstraction by OH radicals) six-member ring cyclitols+aldehydes ketones, etc. →a class of fulvene (isomerization)→ CO_2 +H_2O.
[63]	Mesoporous TiO_2	Benzene	-	-	Benzene is mainly degraded by photo-generated electron-hole pairs and hydroxyl radicals.
[64]	Graphite-SiO_2-TiO_2	Benzene	The graphite-SiO_2-TiO_2 composites exhibited higher photocatalytic activity for degradation of benzene gas under visible light irradiation than that of pure TiO_2.	-	Optimum concentration of graphite facilitates the separation of photogenerated electron–hole pairs for graphite-SiO_2-TiO_2 composites by visible light.
[77]	$LaFeO_3$/black-TiO_2	Toluene	The removal efficiency of black-TiO_2 and $LaFeO_3$ for toluene was 89% and 98%, respectively, and the removal efficiency for IPA was 90% and 94%, respectively.	-	Cat.+photon (the wavelength shorter than 440 nm)→ electrons +O_2→O^{2-}, O^{2-}+toluene and IPA →CO_2+$H_2O_{(g)}$.
[78]	Pd/CeO_2/γ-Al_2O_3	Toluene Acetone Ethyl acetate	T_{98}: 205 °C 220 °C 275 °C	-	-
[79]	CuO/ZnO nanocomposite photocatalysts	Toluene Iopropanol	-	-	Photooxidative activity and stability over ZnO are improved by loading CuO.
[86]	TiO_2	Formaldehyde acetaldehyde	TiO_2 degraded almost 100% of formaldehyde or acetaldehyde at a starting concentration of 400–500 ppb with a relative humidity of 40%.	-	The rate-determining step is the adsorption (external diffusion) on the catalysts active sites, thus the higher the surface area, the higher the degradation.
[88]	g-C_3N_4	Benzoquinone Hydroquinone catechol	-	-	OH radicals+phenol→dihydroxycyclohexadienyl radical adducts→phenoxy radicals→H_2O (a very slow process), adducts+dissolved O_2→dihydroxy intermediates (-HO_2) →CO_2+H_2O.

Table 9. *Cont.*

Refer	Catalyst	VOCs	Catalytic Performance	Remarks	Catalytic Mechanism
[98]	La^{3+}-TiO_2 and Nd^{3+}-TiO_2	VOCs mixture	1.2% La^{3+}-TiO_2 had the highest photocatalytic activity.	-	-
[99]	TiO_2/Pd	VOCs	The conversion rate of VOCs reached 90% when the residence time was 27 s.	-	-
[102]	Mn/ZSM-5	O_3	O_3 can be efficiently decomposed by the Mn/ZSM-5 and used for benzene degradation through the OZCO.	-	Benzene+•OH→phenol→benzoquinone →CO_2 +H_2O.
[100]	Meso-TiO_2/hydro-CF	VOCs	-	-	Promotion effects on degradation of gaseous polar acetone come from well crystallized anatase nanocrystals, hydro-CF skeleton for adsorption, and fast mass transportation within the hierarchical frameworks.

4.3. Non-Thermal Plasma Process

In the non-thermal plasma process, electrons and their surroundings are not in a thermal equilibrium, so the electrons are heated by electric discharges instead of the gas itself, and produce the electrons with high energy, active radicals and ions which can promote numerous chemical reactions in the ionized zones. It can be used to treat the high flow for both low (<100 ppmv) and high (>1000 ppmv) concentrations of VOCs, including toluene, benzene, acetone, trichloroethylene, etc. (Table 10) [47]. The main bottlenecks for the commercialization of the technology are the formation of poison byproducts and high energy consumption. The discharge methods are important for the VOCs removal efficiency, which includes corona discharge, surface discharge, microwave discharge, dielectric barrier discharge, and packed bed dielectric barrier discharge [190–194]. Among these discharge types, the packed bed dielectric barrier discharge shows the most potential in the industry application [195]. Savita K. P. Veerapandian et al. reviewed the packed bed DBD [47]. The influences of dielectric constant, packing materials size, shape, surface properties, and the byproducts formation were discussed.

Using porous and catalytic materials as the packed bed can increase the resistant time of VOCs and decrease the unwanted byproducts, such as O_3, NO_x, and CO (Figure 16) [196]. The packed bed materials can be non-catalytic porous materials, such as activated carbon, porous Al_2O_3, glass, zeolite, graphene oxide, and the catalysts, such as metal oxides, noble metal loaded metal oxides, and catalytic porous materials [197]. For example, using Al_2O_3 as the packed bed can concentrate VOCs molecules on its surface and weaken the bond energy of VOCs, which can enhance the dissociation when these adsorbed molecules encounter the active species in the plasma and increase the collision probability and deep oxidation of VOCs [198]. Lee et al. used porous γ-Al_2O_3 as the packed bed to oxidize toluene to CO_2. It showed a 100% conversion of toluene and high CO_2 selectivity [199]. Gandhi's research results showed that a large surface area and pore volume of alumina can not only increase the conversion of ethylene to CO_2 or CO, but also decrease the selectivity of unwanted byproducts, such as acetaldehyde, acetylene, methane, N_2O, and O_3 [200]. Other researches also showed the same phenomenon in the abatement of benzene, acetone, formaldehyde, TCE, chlorobenzene in non-thermal plasma with the packed bed which has a large surface area and pore volume, such as porous alumina, TiO_2, zeolite, and porous metal oxides [199,201–203]. Due to the large surface area, the retention time and concentration of VOCs molecules increased which led to the increase of collisions between VOCs and active species [200], the adsorption effect can weaken the chemical bond of VOCs [204], and form micro-discharges in the micro-pores in addition to the micro-discharges in the gas phase.
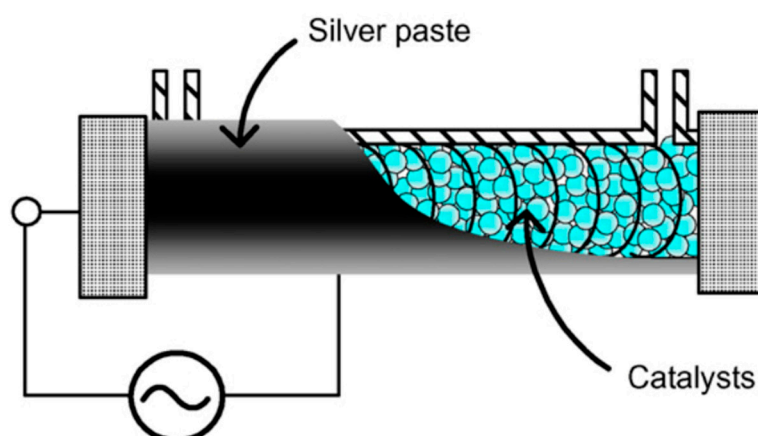
Figure 16. Schematic diagram of the plasma-driven catalyst (PDC) reactor. Reprinted with permission from [196], 2007, Elsevier Ltd.

The addition of catalysts in the non-thermal plasma process as the packed bed can enhance the VOCs removal efficiency significantly due to the plasma assisted reactions on the surface of the catalyst.

These plasma-assisted reactions can generate some active radical species, such as intermediates with electrons, $O\cdot$, $OH\cdot$, $N_2\cdot$, $NO\cdot$, $N_2O\cdot$ in the gas phase and $O\cdot$, $OH\cdot$ on the surface of catalysts, which can improve the VOCs removal efficiency and increase the CO_x selectivity [80]. The catalysts include metal oxides, such as CuO, MnO_2, CeO_2, NiO, CoO_2, and Fe_2O_3, and noble metals, such as Pt, Au, and Ag [65,196,203,205–209]. The different kinds of oxygen species in catalysts, namely lattice oxygen, surface oxygen, and absorbed oxygen, are very helpful for the oxidation of VOCs, which can activate the oxygen molecules in the gas phase. P.J. Asilevi et al. established a laboratory scale DBD reactor for the removal of toluene by $\cdot O$ and $\cdot OH$ which were generated from the reaction between O_2 and H_2O and the removal efficiency of VOCs can be improved by increasing the oxygen concentration and relative humidity [210]. Lu et al. used FeO_x/SBA-15 as the packed bed to eliminate toluene in the non-thermal plasma process. The results showed that the presence of Fe^{2+} can increase the toluene removal efficiency and CO_x selectivity obviously and reduce the formation of unwanted and toxic byproducts [80]. Zhu et al. prepared 5 wt% CuO/-Al_2O_3 as the packed bed to the abatement acetone. It showed better performance than the one without CuO due to the better reducibility and abundant active oxygen species [87]. Li et al. prepared Pt/Al_2O_3 and it showed higher decomposition efficiency than the unloaded Al_2O_3 due to the presence of Pt, which increases the number of active sites and reduces the activation energy of the decomposition reaction and suppresses harmful NO_x formation [65]. The research by Hua Song et al. showed that $CoMnO_x$/TiO_2 can obviously improve the plasma removal of VOCs [103].

There are other factors that influence the VOCs removal efficiency, such as humidity and the plasma structure. In industrial conditions, the humidity in the VOCs stream is the factor which must be considered. The humidity has both a positive and negative effect on the removal of VOCs in the non-thermal plasma process. The water molecules can modify the surface of the packed bed, especially the catalytic packed bed, quench the free electrons and active species, and produce OH radicals during the discharge process [103,202,207,211,212]. A lot of studies showed that the presence of humidity can reduce the VOCs removal efficiency by quenching the high energy electrons and reactive species, and modify the catalysts surface ($BaTiO_3$) in the decomposition of toluene, benzene, xylene, and C_2F_2 [103,207,212]. On the other hand, the humidity can suppress the formation of toxic byproducts, such as CO and NOx by deactivation of some oxygen species in the catalysts [213,214]. The optimization of the plasma structure also can enhance the VOCs decomposition efficiency. Muhammad Farooq Mustafa et al. designed a double dielectric barrier discharge reactor, in which the conversion of tetrachloroethylene, toluene, trichloroethylene, benzene, ethyl acetate, and carbon disulfide can be 100% with $BaTiO_3$ and HZSM-5 as catalysts, respectively [215].

There are also some disadvantages in the non-thermal plasma process, such as high energy consumption, low VOCs conversion (mostly about 30% to 70%), low CO_x selectivity, and produced unwanted byproducts. The other barrier for the application of non-thermal plasma in the industry is the high cost and the high energy consumption. The way to solve these problems is the development of a highly efficient catalytic packed bed and the optimization of an electrode structure.

Table 10. Catalysts for VOCs elimination through the non-thermal plasma process.

Refer	Catalyst	VOCs	Catalytic Performance	Remarks	Catalytic Mechanism
[65]	Pt/Al_2O_3	Benzene byproducts	-	-	-
[80]	$FeO_x/SBA-15$	Toluene	-	Under the condition of 3% Fe loading, the oxidation of toluene is the best one.	(1) Direct removal caused by the collision of electrons or oxidation caused by the gas-phase radicals ($O\bullet$, $OH\bullet$, $N_2\bullet$, $NO\bullet$, $NO_2\bullet$) in the gas phase; (2) the reaction between adsorbed toluene or other intermediates and the active species ($O\bullet$, $OH\bullet$) on the catalyst surface. O_2 might be fixed on the catalyst surface via a facile interconversion between Fe^{2+} and Fe^{3+} states and then be transported to the toluene or intermediates leading to CO_2 formation.
[87]	$CuO/g-Al_2O_3$	Ccetone	-	5.0 wt% $CuO/g-Al_2O_3$ catalyst has the highest removal rate of acetone, reaching 67.9%.	Both short-lived radicals and acetone/intermediates can be adsorbed on the catalyst surfaces to initiate a series of surface oxidation reactions, forming CO, CO_2, H_2O, and byproducts.
[103]	$CoMnO_x/TiO_2$	O_3	-	When the temperature is 320 °C, the decomposition efficiency of O_3 is 98%.	-

4.4. Electron Beam Treatment

In the electron beam technology, an electron beam generated from an EB accelerator and absorbed by the background gas to ionize the air and form some active oxidizing radicals, such as ·OH and ·HO$_2$ and excited ions as O (^{3}P), which is critical for the destruction of VOCs [216–218]. The oxidizing radicals reacted with VOCs and decomposed them to inorganic compounds. There are three types of accelerators used for VOCs decomposition, including transformer accelerator, ultrahigh frequency accelerator, and linear microwave accelerator [217]. This technology has been used for the elimination of acetaldehyde, benzene, dodecane, ethylbenzene, hexadecane, pentane, styrene, tetradecane, toluene, trimethylamine, turpentine, xylene, dimethyl sulfide, dimethyl disulfide, methyl mercaptan, and chlorinated VOCs in a lab or pilot scale [218–228]. The electron beam can treat the waste gas with a low concentration of VOCs (10 to hundreds ppm). The initial electrons from an electron beam can hardly decompose the VOCs molecules, while it can react with background gases and form active radicals. The way to improve the abatement rate of aromatic VOCs includes the addition of humidity (formation of OH·), ammonia, chlorinated VOCs, ozone, and using an absorbed dose [220,229]. The reaction temperature, VOCs molecular structure, and background gas also influence the decomposition efficiency. However, there are also some drawbacks of the electron beam technology, the generation of active oxidizing radicals, e.g., ·OH and ·HO$_2$ can lead to the creation of toxic intermediates, especially in the case of the VOCs emission with an unknown composition, such as the production of toxic byproducts (aerosol, ozone, CO, and other trace organic compounds). The equipment is also too complex. It still needs more research for the industrial application.

5. Outlook of the Different Kinds of Technologies

Different kinds of VOCs were emitted from different parts of pharmaceutical production processes. With the new VOCs discharge standards coming into force, it is critical for the pharmaceutical companies to eliminate VOCs exhaustively in China. According to the production processes and conditions, the suitable VOCs elimination technologies must be selected with the highest efficiency and at the lowest cost. Adsorption, absorption, incineration, catalytic combustion, biodegradation, and non-thermal plasma technologies have been applied in factories for the abatement of VOCs. Adsorption and absorption are commonly the first used methods to recycle useful VOCs. Then, the rest of the VOCs were decomposed by other technologies, such as incineration, catalytic combustion, non-thermal plasma, biodegradation, and non-thermal plasma. The key point for the improvement of catalytic combustion and non-thermal plasma is the development of efficient catalysts or packed bed materials. Some new technologies are emerging for the abatement of VOCs, such as photocatalysis and electron beam radiation. These new technologies have shown good potential for the elimination of VOCs with a high efficiency and low energy cost. However, they still have some engineering problems for the industrial application. It is important to develop VOCs elimination technologies to decrease the amounts of VOCs in the discharged waste gas. The final solution for the VOCs is avoiding the emission of VOCs from the whole pharmaceutical production processes by developing new chemical and engineering technologies for the production of medicine.

Conflicts of Interest: The authors declare no conflict of interest.

References

1. Li, W.B.; Wang, J.X.; Gong, H. Catalytic combustion of VOCs on non-noble metal catalysts. *Catal. Today* **2009**, *148*, 81–87. [CrossRef]

2. Muhammad, S.K.; Shaikh, A.R.; Mohammad, M.H. Catalytic oxidation of volatile organic compounds (VOCs): A review. *Atmos. Environ.* **2016**, *140*, 117–134.

3. Cheng, G. Study on VOCs Emissions Research Present Situation and the Emission Reduction Potential of Key Industries in Hebei Province. Master's Thesis, Hebei University of Science and Technology, Shijiangzhuang, China, 2016.

4. Li, Y. Study on Emission Standard of Air Pollutants for Pharmaceutical Industry Chemical Synthesis Products Category. Master's Thesis, Zhejiang University of Technology, Hangzhou, China, 2016.

5. Atkinson, R. Gas-phase tropospheric chemistry of volatile organic compounds: 1. Alkanes and alkenes. *J. Phys. Chem. Ref. Data* **1997**, *26*, 215–229. [CrossRef]

6. Fontane, H.; Veillerot, M.; Gallo, J.C.; Guillermo, R. *8th International Symposium on Transport and Air Pollution*; Verlag der Technischen Universität Graz: Graz, Austria, 1999.

7. Rivière, E. *CITEPA Report*; Fieldwork Inhabitants: Paris, France, 1998.

8. Duncan, B.N.; Yoshida, Y.; Olson, J.R.; Sillman, S.; Martin, R.V.; Lamsal, L.; Hu, Y.; Pickering, K.E.; Retscher, C.; Allen, D.J.; et al. Application of OMI observations to a space-based indicator of NOx and VOC controls on surface ozone formation. *Atmos. Environ.* **2010**, *44*, 2213–2223. [CrossRef]

9. Atkinson, R. Atmospheric chemistry of VOCs and NO_x. *Atmos. Environ.* **2000**, *34*, 2063–2101.

10. National Bureau of Statistics of the People's Republic of China. Available online: http://www.stats.gov.cn/tjsj/ (accessed on 26 May 2020).

11. Chen, Y. Study on Current and Future Industrial Emission of Volatile Organic Compounds in China. Master's Thesis, South China University of Technology, Guangzhou, China, 2011.

12. Huang, W. Characteristics of Industrial VOCs Emissions and Evaluation of Control Technology in China. Master's Thesis, Zhejiang University, Hangzhou, China, 2016.

13. Ministry of Ecological Environment of the People's Republic of China. *Standards for Emissions of Atmospheric Pollutants from Pharmaceutical Industry (Draft for Comments)*; Ministry of Ecological Environment of the People's Republic of China: Beijing, China, 2017.

14. Lu, Y. Establishment and Application on Assessment System of VOCs's Control Technology of Pharmaceutical Industry. Master's Thesis, Hebei University of Science and Technology, Shijiazhuang, China, 2016.

15. Hu, G. Research of Emission and Control Technology of VOCs and Odorous Gas from Pharmacy Industry in China. Master's Thesis, Nankai University, Tianjing, China, 2013.

16. Li, X. The System of Discharge Standards of Pollutants for Pharmaceutical Industry and a case Study. Master's Thesis, The Chinese Research Academy of Environmental Science, Beijing, China, 2006.

17. He, J. *Fermentology*; China Medical Science Press: Beijing, China, 2009.

18. Wang, Y. *Chemical Pharmaceutical Technology*; Chemical Industry Press: Beijing, China, 2008.

19. Zhou, T.; Ma, Q.; Chen, H. Treatment of chemical synthesized pharmaceutical wastewater by hybrid biological reactor. *Ind. Water Wastewater* **2010**, *41*, 42–45.

20. Chen, P. *Pharmaceutical Technology*; Hubei Science and Technology Press: Wuhan, China, 2008.

21. Qi, X. *Modern Biopharmaceutical Technology*; Chemical Industry Press: Beijing, China, 2009.

22. Cao, G. *Pharmaceutical Engineering of Traditional Chinese Medicine*; Chemical Industry Press: Beijing, China, 2004.

23. Wu, C. The thinking and Countermeasures for the Structuring of Learning Seals Team in Chengdu Zhonghui Pharmaceuticals Company. Master's Thesis, Southwestern University of Finance and Economics, Chengdu, China, 2006.

24. Chen, Y.; Ye, D.; Liu, X.; Wu, J.; Huang, B.; Zheng, Y. Source tracing and characteristics of industrial VOCs emissions in China. *Chin. Environ. Sci.* **2012**, *32*, 48–55.

25. Song, J. Studies on the Adsorption of VOCs by Activated Carbons and the Structure-Function Relationship. Ph.D. Thesis, Central South University, Changsha, China, 2014.

26. Khan, F.I.; Ghoshal, A.K. Removal of Volatile Organic Compounds from polluted air. *J. Loss Prevent. Proc. Ind.* **2000**, *13*, 527–545. [CrossRef]

27. Parmar, G.R.; Rao, N.N. Emerging Control Technologies for Volatile Organic Compounds. *Crit. Rev. Environ. Sci. Technol.* **2009**, *39*, 41–78. [CrossRef]

28. Shah, R.; Thonon, B.; Benforado, D. Opportunities for heat exchanger applications in environmental systems. *Appl. Therm. Eng.* **2000**, *20*, 631–650. [CrossRef]

29. Dunn, R.F.; El-Halwagi, M.M. Selection of Optimal VOC-condensation Systems. *Waste Manag.* **1994**, *14*, 103–113. [CrossRef]

30. Huang, W.; Shi, L.; Hu, Z.; Zheng, Z. Integrated technology of condensation and adsorption for volatile organic compounds recovery. *Chem. Eng.* **2012**, *6*, 13–17.

31. Zhang, X.; Gao, B.; Creamer, A.E.; Cao, C.; Li, Y. Adsorption of VOCs onto engineered carbon materials: A review. *J. Hazard. Mater.* **2017**, *338*, 102–123. [CrossRef]

32. Wang, S.; Zhang, L.; Long, C.; Li, A. Enhanced adsorption and desorption of vocs vapor on novel micro-mesoporous polymeric adsorbents. *J. Coll. Interface Sci.* **2014**, *428*, 185–190. [CrossRef] [PubMed]

33. Serna-Guerrero, R.; Sayari, A. Applications of pore-expanded mesoporoussilica 7, Adsorption of volatile organic compounds. *Environ. Sci. Technol.* **2007**, *41*, 4761–4766. [CrossRef] [PubMed]

34. U.S. Environmental Protection Agency Clean Air Technology Center. Choosing an adsorption system for VOC: Carbon, zeolite, or polymers? In Proceedings of the SPIE—The International Society for Optical Engineering, Research Triangle Park, NC, USA, 1 May 1999.

35. Kujawa, J.; Cerneaux, S.; Kujawski, W. Removal of hazardous volatile organic compounds from water by vacuum pervaporation with hydrophobic ceramic membranes. *J. Membr. Sci.* **2015**, *474*, 11–19. [CrossRef]

36. Li, Y.X.; Chen, J.Y.; Sun, Y.H. Adsorption of multicomponent volatile organic compounds on semi-coke. *Carbon* **2008**, *46*, 858–863.

37. Komori. Preparation of N-acetylmorpholine. *J. Chem. Soc. Jpn. Ind. Chem.* **1959**, *62*, 220–225.

38. Chang, F.T.; Lin, Y.C.; Bai, H.; Pei, B.S. Adsorption and desorption characteristics of semiconductor volatile organic compounds on the thermal swing honeycomb zeolite concentrator. *J. Air Waste Manage. Assoc.* **2003**, *53*, 1384–1390. [CrossRef]

39. Liu, Y. Study on Ceramic Honeycomb Monolithic Adsorbents for VOCs Adsorption. Master's Thesis, South China University of Technology, Guangzhou, China, 2015.

40. Moretti, E.C. Reduce VOC and HAP emissions. *Chem. Eng. Prog.* **2002**, *98*, 30–40.

41. Everaert, K.; Baeyens, J. Catalytic combustion of volatile organic compounds. *J. Hazard. Mater.* **2004**, *B109*, 113–139. [CrossRef]

42. Liotta, L.F. Catalytic oxidation of volatile organic compounds on supported noble metals. *Appl. Catal. B Environ.* **2010**, *100*, 403–412. [CrossRef]

43. Spivey, J.J. Complete Catalytic Oxidation of Volatile Organics. *Ind. Eng. Chem. Res.* **1987**, *26*, 2165–2180. [CrossRef]

44. Zhang, Z.; Jiang, Z.; Shangguan, W. Low-temperature catalysis for VOCs removal in technology andapplication: A state-of-the-art review. *Catal. Today* **2016**, *264*, 270–278. [CrossRef]

45. Barbusinski, K.; Kalemba, K.; Kasperczyk, D.; Urbaniec, K.; Kozik, V. Biological methods for odor treatment: A review. *J. Clean. Prod.* **2017**, *152*, 223–241. [CrossRef]

46. Mudliar, S.; Giri, B.; Padoley, K.; Satpute, D.; Dixit, R.; Bhatt, P.; Pandey, R.; Juwarkar, A.; Vaidya, A. Bioreactors for treatment of VOCs and odours—A review. *J. Environ. Manage.* **2010**, *91*, 1039–1054. [CrossRef]

47. Veerapandian, S.K.P.; Leys, C.; Geyter N., D.; Morent, R. Abatement of VOCs using packed bed non-thermal plasma reactors: A review. *Catalysts* **2017**, *7*, 113. [CrossRef]

48. Son, Y.S. Decomposition of VOCs and odorous compounds by radiolysis: A critical review. *Chem. Eng. J.* **2017**, *316*, 609–622. [CrossRef]

49. Wang, H. Study on Removal of Miced VOCs in Air by Dielectric Barrier Discharge. Ph.D. Thesis, Dalian University of Technology, Dalian, China, 2009.

50. Hao, J. Control Study of VOCs Regioned Joint Prevention and Control of Atmospheric Pollution. Master's Thesis, Hebei University of Technology, Shijiazhuang, China, 2012.

51. Xi, J.; Wu, J.; Hu, H.; Wang, C. Application status of industrial VOCs gas treatment techniques. *China Environ. Sci.* **2012**, *32*, 1955–1960.

52. Hao, Y. Study on The Pharmaceutical and Chemical Industry VOCs and Odor Pollution Characteristics. Master's Thesis, Hebei University of Science and Technology, Shijiazhung, China, 2014.

53. Department of Environmental Protection of Zhejiang Province. *Standards for Emissions of Atmospheric Pollutants from Pharmaceutical Industry in Zhejiang Province*; Department of Environmental Protection of Zhejiang Province: Hangzhou, Chain, 2015–2016.

54. Salar-García, M.J.; Ortiz-Martínez, V.M.; Hernández-Fernández, F.J.; de los Ríos, A.P.; Quesada-Medina, J. Ionic liquid technology to recover volatile organic compounds (VOCs). *J. Hazard. Mater.* **2017**, *321*, 484–499. [CrossRef]

55. Minella, M.; Baudino, M.; Minero, C. A revised photocatalytic transformation mechanism for chlorinated VOCs: Experimental evidence from C_2Cl_4 in the gas phase. *Catal. Today* **2018**, *313*, 114–121. [CrossRef]

56. Papaefthimiou, P.; Ioannides, T.; Verykios, X.E. Combustion of non-halogenated volatile organic compounds over group VIII metal catalysts. *Appl. Catal. B Environ.* **1997**, *13*, 175–184. [CrossRef]

57. Tabakova, T.; Ilieva, L.; Petrova, P. Complete benzene oxidation over mono and bimetallic Au–Pd catalysts supported on Fe-modified ceria. *Chem. Eng. J.* **2015**, *260*, 133–141. [CrossRef]

58. Wang, Y.; Yang, D.; Li, S.; Zhang, L.; Zheng, G.; Guo, L. Layered copper manganese oxide for the efficient catalytic CO and VOCs oxidation. *Chem. Eng. J.* **2018**, *357*, 258–268. [CrossRef]

59. Alifanti, M.; Florea, M.; Pârvulescu, V.I. Ceria-based oxides as supports for $LaCoO_3$ perovskite catalysts for total oxidation of VOC. *Appl. Catal. B Environ.* **2007**, *70*, 400–405. [CrossRef]

60. Spinicci, R.; Faticanti, M.; Marini, P.; De Rossi, S.; Porta, P. Catalytic activity of $LaMnO_3$ and $LaCoO_3$ perovskites towards VOCs combustion. *J. Mol. Catal. A Chem.* **2003**, *197*, 147–155. [CrossRef]

61. Liu, L.; Li, J.; Zhang, H.; Li, L.; Zhou, P.; Meng, X.; Guo, M.; Jia, J.; Sun, T. In situ fabrication of highly active γ-MnO_2/$SmMnO_3$ catalyst for deep catalytic oxidation of gaseous benzene, ethylbenzene, toluene, and o-xylene. *J. Hazard. Mater.* **2019**, *362*, 178–186. [CrossRef]

62. Shu, Y.; Ji, J.; Xu, Y.; Deng, J.; Huang, H.; He, M.; Leung, D.Y.C.; Wu, M.; Liu, S.; Liu, S.; et al. Promotional role of Mn doping on catalytic oxidation of VOCs over mesoporous TiO_2 under vacuum ultraviolet (VUV) irradiation. *Appl. Catal. B Environ.* **2018**, *220*, 78–87. [CrossRef]

63. Ji, J.; Xu, Y.; Huang, H.; He, M.; Liu, S.; Liu, G.; Xie, R.; Feng, Q.; Shu, Y.; Zhan, Y.; et al. Mesoporous TiO_2 under VUV irradiation: Enhanced photocatalytic oxidation for VOCs degradation at room temperature. *Chem. Eng. J.* **2017**, *327*, 490–499. [CrossRef]

64. Yadav, H.M.; Jung, S.C.; Kim, J.S. Visible light photocatalyticperformance of in situ synthesized graphite-SiO_2–TiO_2 composite towards degradation of benzene gas. *J. Nanosci. Nanotechnol.* **2018**, *18*, 2032–2036. [CrossRef]

65. Li, J.; Han, S.; Bai, S.; Han, S.; Song, H.; Pu, Y.; Zhu, X.; Chen, W. Effect of Pt/gamma-Al_2O_3 catalyst on nonthermal plasma decomposition of benzene and byproducts. *Environ. Eng. Sci.* **2011**, *28*, 395–403. [CrossRef]

66. Pei, W.; Liu, Y.; Deng, J.; Zhang, K.; Hou, Z.; Zhao, X.; Dai, H. Partially embedding Pt nanoparticles in the skeleton of 3DOM Mn_2O_3: An effective strategy for enhancing catalytic stability in toluene combustion. *Appl. Catal. B Environ.* **2019**, *256*, 117814–117824. [CrossRef]

67. Hosseini, M.; Barakat, T.; Cousin, R. Catalytic performance of core–shell and alloy Pd–Au nanoparticles for total oxidation of VOC: The effect of metal deposition. *Appl. Catal. B Environ.* **2012**, *111*, 218–224. [CrossRef]

68. Lee, D.S.; Chen, Y.W. The mutual promotional effect of Au–Pd/CeO_2 bimetallic catalysts on destruction of toluene. *J. Taiwan Ins. Chem. Eng.* **2013**, *44*, 40–44. [CrossRef]

69. Yang, X.; Yu, X.; Lin, M.; Ma, X.; Ge, M. Enhancement effect of acid treatment on Mn_2O_3 catalyst for toluene oxidation. *Catal. Today* **2019**, *327*, 254–261. [CrossRef]

70. Huang, H.; Liu, Y.; Tang, W.; Chen, Y. Catalytic activity of nanometer $La_{1-x}Sr_xCoO_3$ (x = 0, 0.2) perovskites towards VOCs combustion. *Catal. Commun.* **2008**, *9*, 55–59. [CrossRef]

71. Suárez-Vázquez, S.I.; Gil, S.; García-Vargas, J.M.; Cruz-López, A.; Giroir-Fendler, A. Catalytic oxidation of toluene by $SrTi_{1-X}BXO_3$ (B = Cu and Mn) with dendritic morphology synthesized by one pot hydrothermal route. *Appl. Catal. B Environ.* **2018**, *223*, 201–208. [CrossRef]

72. Guo, M.; Li, K.; Liu, L.; Zhang, H.; Hu, X.; Min, X.; Jia, J.; Sun, T. Resource utilization of spent ternary lithium-ions batteries: Synthesis of highly active manganese-based perovskite catalyst for toluene oxidation. *J. Taiwan Inst. Chem. Eng.* **2019**, *102*, 268–275. [CrossRef]

73. Yang, J.; Li, L.; Yang, X.; Song, S.; Li, J.; Jing, F.; Chu, W. Enhanced catalytic performances of in situ-assembled $LaMnO$ /δ-MnO_2, hetero-structures for toluene combustion. *Catal. Today* **2019**, *327*, 19–27. [CrossRef]

74. Sihaib, Z.; Puleo, F.; Pantaleo, G.; Parola, V.L.; Valverde, J.L.; Gil, S.; Liotta, L.F.; Giroir-Fendler, A. The effect of citric acid concentration on the properties of LaMnO$_3$ as a catalyst for hydrocarbon oxidation. *Catalysts* **2019**, *9*, 226. [CrossRef]

75. Peng, Y.; Zhang, L.; Chen, L.; Yuan, D.; Wang, G.; Meng, X.; Xiao, F.S. Catalytic performance for toluene abatement over Al-rich Beta zeolite supported manganese oxides. *Catal. Today* **2017**, *297*, 182–187. [CrossRef]

76. Qin, Y.; Qu, Z.; Dong, C.; Wang, Y.; Huang, N. Highly catalytic activity of Mn/SBA-15 catalysts for toluene combustion improved by adjusting the morphology of supports. *J. Environ. Sci.* **2019**, *76*, 208–216. [CrossRef]

77. Lee, Y.E.; Chung, W.C.; Chang, M.B. Photocatalytic oxidation of toluene and isopropanol by LaFeO3/black-TiO$_2$. Environ. *Sci. Pollut. Res.* **2019**, *26*, 20908–20919. [CrossRef]

78. Bettini, S.; Pagano, R.; Semeraro, P.; Ottolini, M.; Salvatore, L.; Marzo, F.; Lovergine, N.; Giancane, G.; Valli, L. SiO$_2$-Coated ZnO Nanoflakes Decorated with Ag Nanoparticles for Photocatalytic Water Oxidation. *Chem. Eur. J.* **2019**, *25*, 14123–14132. [CrossRef] [PubMed]

79. Li, Z.; Pan, X.; Yi, Z. Photocatalytic oxidation of methane over CuO-decorated ZnO nanocatalysts. *J. Mater. Chem. A* **2019**, *7*, 469–475. [CrossRef]

80. Lu, M.; Huang, R.; Wu, J.; Fu, M.; Chen, L.; Ye, D. On the performance and mechanisms of toluene removal by FeO$_x$/SBA-15-assisted non-thermal plasma at atmospheric pressure and room temperature. *Catal. Today* **2015**, *242*, 274–286. [CrossRef]

81. Nevanperä, T.K.; Ojala, S.; Laitinen, T.; Pitkäaho, S.; Saukko, S.; Keiski, R.L. Catalytic Oxidation of Dimethyl Disulfide over Bimetallic Cu–Au and Pt–Au Catalysts Supported on γ-Al$_2$O$_3$, CeO$_2$, and CeO$_2$–Al$_2$O$_3$. *Catalysts* **2019**, *9*, 603. [CrossRef]

82. Rotter, H.; Landau, M.; Herskowitz, M. Combustion of chlorinated VOC on nanostructured chromia aerogel as catalyst and catalyst support. *Environ. Sci. Technol.* **2005**, *39*, 6845–6850. [CrossRef]

83. Dai, Q.; Wang, X.; Lu, G. Low-temperature catalytic destruction of chlorinated VOCs over cerium oxide. *Catal. Commun.* **2007**, *8*, 1645–1649. [CrossRef]

84. Ikhlaq, A.; Kasprzyk-Hordern, B. Catalytic ozonation of chlorinated VOCs on ZSM-5 zeolites and alumina: Formation of chlorides. *Appl. Catal. B Environ.* **2017**, *200*, 274–282. [CrossRef]

85. Fei, Z.; Cheng, C.; Chen, H.; Li, L.; Yang, Y.; Liu, Q.; Chen, X.; Zhang, Z.; Tang, J.; Cui, M.; et al. Construction of uniform nanodots CeO$_2$ stabilized by porous silica matrix for 1,2-dichloroethane catalytic combustion. *Chem. Eng. J.* **2019**, *370*, 916–924. [CrossRef]

86. Stucchi, M.; Galli, F.; Bianchi, C.L.; Pirola, C.; Boffito, D.C.; Biasioli, F.; Capucci, V. Simultaneous photodegradation of VOC mixture by TiO$_2$ powders. *Chemosphere* **2018**, *193*, 198–206. [CrossRef] [PubMed]

87. Zhu, X.; Tu, X.; Mei, D.; Zheng, C.; Zhou, J.; Gao, X.; Luo, Z.; Ni, M.; Cen, K. Investigation of hybrid plasma-catalytic removal of acetone over CuO/-Al$_2$O$_3$ catalysts using response surface method. *Chemosphere* **2016**, *155*, 9–17. [CrossRef] [PubMed]

88. Li, Z.; Meng, X.; Zhang, Z. Fabrication of surface hydroxyl modified g-C$_3$N$_4$ with enhanced photocatalytic oxidation activity. *Catal. Sci. Technol.* **2019**, *9*, 3979–3993. [CrossRef]

89. Wu, Y.; Shi, S.; Yuan, S.; Yuan, S.; Bai, T.; Xing, S. Insight into the enhanced activity of Ag/NiO$_x$-MnO$_2$ for catalytic oxidation of o-xylene at low temperatures. *Appl. Surf. Sci.* **2019**, *479*, 1262–1269. [CrossRef]

90. Yang, S.; Zhao, H.; Dong, F.; Zha, F.; Tang, Z. Highly efficient catalytic combustion of o-dichlorobenzene over three-dimensional ordered mesoporous cerium manganese bimetallic oxides: A new concept of chlorine removal mechanism. *Mol. Catal.* **2019**, *463*, 119–129. [CrossRef]

91. He, D.; Zhao, Y.; Yang, S.; Mei, Y.; Yu, J.; Liu, J.; Chen, D.; He, S.; Luo, Y. Enhancement of catalytic performance and resistance to carbonaceous deposit of lanthanum (La) doped HZSM-5 catalysts for decomposition of methyl mercaptan. *Chem. Eng. J.* **2018**, *336*, 579–586. [CrossRef]

92. Liu, N.; Shi, D.; Zhang, R.; Li, Y.; Chen, B. Highly selective catalytic combustion of acrylonitrile towards nitrogen over Cu-modified zeolites. *Catal. Today* **2018**, *332*, 201–213. [CrossRef]

93. Fiorenza, R.; Crisafulli, C.; Condorelli, G.G.; Lupo, F.; Scire, S. Au–Ag/CeO$_2$ and Au–Cu/CeO$_2$ Catalysts for Volatile Organic Compounds Oxidation and CO Preferential Oxidation. *Catal. Lett.* **2015**, *145*, 1691–1702. [CrossRef]

94. Yao, J.; Lu, H.; Xiao, Y.; Hou, B.; Li, D.; Jia, L. Sub-molten salt-acid treatment of LaCoO$_3$ for a highly active catalyst towards propane combustion. *Catal. Commun.* **2019**, *128*, 10578–10583. [CrossRef]

95. Zhang, K.; Peng, X.; Yang, H.; Wang, X.; Zhang, Y.; Zheng, Y.; Xiao, Y.; Jiang, L. Effect of MnO$_2$ morphology on its catalytic performance in lean methane combustion. *Mater. Res. Bull.* **2018**, *111*, 338–341. [CrossRef]

96. Wei, Y.; Ni, L.; Li, M.; Zhao, J. A template-free method for preparation of MnO_2 catalysts with high surface areas. *Catal. Today* **2017**, *297*, 188–192. [CrossRef]

97. Sinquin, G.; Petit, C.; Hindermann, J.P.; Kiennemann, A. Study of the formation of $LaMO_3$ (M = Co, Mn) perovskites by propionates precursors: Application to the catalytic destruction of chlorinated VOCs. *Catal. Today* **2001**, *70*, 183–196. [CrossRef]

98. Alberici, R.M.; Jardim, W.F. Photocatalytic destruction of VOCs in the gas-phase using titanium dioxide. *Appl. Catal. B Environ.* **1997**, *14*, 55–68. [CrossRef]

99. Fujimoto, T.M.; Ponczek, M.; Rochetto, U.L.; Landers, R.; Tomaz, E. Photocatalytic oxidation of selected gas-phase VOCs using UV light, TiO_2, and TiO_2/Pd. *Environ. Sci. Pollut. Res.* **2017**, *24*, 6390–6396. [CrossRef]

100. Qian, X.; Ren, M.; Yue, D.; Zhu, Y.; Han, Y.; Bian, Z.; Zhao, Y. Mesoporous TiO_2 films coated on carbon foam based on waste polyurethane for enhanced photocatalytic oxidation of VOCs. *Appl. Catal. B Environ.* **2017**, *212*, 1–6. [CrossRef]

101. Zhang, L.; Peng, Y.; Zhang, J.; Chen, L.; Meng, X.; Xiao, F.S. Adsorptive and catalytic properties in the removal of volatile organic compounds over zeolite-based materials. *Chin. J. Catal.* **2016**, *37*, 800–809. [CrossRef]

102. Huang, H.; Huang, H.; Zhan, Y.; Liu, G.; Wang, X.; Lu, H.; Xiao, L.; Feng, Q.; Leung, D.Y.C. Efficient degradation of gaseous benzene by VUV photolysis combined with ozone-assisted catalytic oxidation: Performance and mechanism. *Appl. Catal. B Environ.* **2016**, *186*, 62–68. [CrossRef]

103. Song, H.; Peng, Y.; Liu, S.; Bai, S.; Hong, X.; Li, J. The Roles of Various Plasma Active Species in Toluene Degradation by Non-thermal Plasma and Plasma Catalysis. *Plasma Chem. Plasma Process.* **2019**, *39*, 1469–1482. [CrossRef]

104. Wang, L.; Wang, C.; Xie, H.; Zhan, W.; Guo, Y. Catalytic combustion of vinyl chloride over Sr doped $LaMnO_3$. *Catal. Today* **2018**, *327*, 190–195. [CrossRef]

105. Kołodziej, A.; Łojewska, J. Optimization of structured catalyst carriers for VOC combustion. *Catal. Today* **2005**, *105*, 378–384. [CrossRef]

106. Joung, H.J.; Kim, J.H.; Oh, J.S.; You, D.W.; Park, H.O.; Jung, K.W. Catalytic oxidation of VOCs over CNT-supported platinum nanoparticles. *Appl. Surf. Sci.* **2014**, *290*, 267–273. [CrossRef]

107. Kim, S.C.; Shim, W.G. Properties and performance of Pd based catalysts for catalytic oxidation of volatile organic compounds. *Appl. Catal. B Environ.* **2009**, *92*, 429–436. [CrossRef]

108. Bedi, J.; Rosas, J.M.; Rodríguez-Mirasol, J.; Cordero, T. Pd supported on mesoporous activated carbons with high oxidation resistance as catalysts for toluene oxidation. *Appl. Catal. B Environ.* **2010**, *94*, 8–18. [CrossRef]

109. Usón, L.; Colmenares, M.G.; Hueso, J.L.; Sebastián, V.; Balas, F.; Arruebo, M.; Santamaría, J. VOCs abatement using thick eggshell Pt/SBA-15 pellets with hierarchical porosity. *Catal. Today* **2014**, *227*, 179–186. [CrossRef]

110. Carrillo, A.M.; Carriazo, J.G. Cu and Co oxides supported on halloysite for the total oxidation of toluene. *Appl. Catal. B Environ.* **2015**, *164*, 443–452. [CrossRef]

111. Kucherov, A.V.; Sinev, I.M.; Ojala, S.; Keiski, R.L.; Kustov, M. Adsorptive-catalytic removal of CH_3OH, CH_3SH, and CH_3SSCH_3 from air over the bifunctional system noble metals/HZSM-5. *Stud. Surf. Sci. Catal.* **2007**, *170*, 1129–1136.

112. Wang, J. Study on Supported Ruthenium Catalysts for the Catalytic Oxidation of VOCs. Ph.D. Thesis, Institute of Process Engineering, CAS, China, 2016.

113. Abdelouahab-Reddam, Z.; Mail, R.E.; Coloma, F.; Sepúlveda-Escribano, A. Platinum supported on highly-dispersed ceria on activated carbon for the total oxidation of VOCs. *Appl. Catal. A Gen.* **2015**, *494*, 87–94. [CrossRef]

114. Piumetti, M.; Fino, D.; Russo, N. Mesoporous manganese oxides prepared by solution combustion synthesis as catalysts for the total oxidation of VOCs. *Appl. Catal. B Environ.* **2015**, *163*, 277–287. [CrossRef]

115. Grbic, B.; Radic, N.; Terlecki-Baricevic, A. Kinetics of deep oxidation of n-hexane and toluene over Pt/Al_2O_3 catalysts: Oxidation of mixture. *Appl. Catal. B Environ.* **2004**, *50*, 161–166. [CrossRef]

116. Patterson, M.J.; Angove, D.E.; Cant, N.W. The effect of carbon monoxide on the oxidation of four C6 to C8 hydrocarbons over platinum, palladium and rhodium. *Appl. Catal. B Environ.* **2000**, *26*, 47–57. [CrossRef]

117. McCabe, R.W.; Mitchell, P.J. Exhaust-catalyst development for methanol-fueled vehicles: 1. A comparative study of methanol oxidation over alumina-supported catalysts containing group 9, 10, and 11 metals. *Appl. Catal.* **1986**, *27*, 83–98. [CrossRef]

118. Liotta, L.F.; Ousmane, M.; Di Carlo, G.; Pantaleo, G.; Deganello, G.; Marcì, G.; Retailleau, L.; Giroir-Fendler, A. Total oxidation of propene at low temperature over Co_3O_4–CeO_2 mixed oxides: Role of surface oxygen vacancies and bulk oxygen mobility in the catalytic activity. *Appl. Catal. A Gen.* **2008**, *347*, 81–88. [CrossRef]

119. Liotta, L.F.; Ousmane, M.; Di Carlo, G.; Pantaleo, G.; Deganello, G.; Boreave, A.; Giroir-Fendler, A. Catalytic removal of toluene over Co_3O_4–CeO_2 mixed oxide catalysts: Comparison with Pt/Al_2O_3. *Catal. Lett.* **2009**, *127*, 270–276. [CrossRef]

120. Mitsui, T.; Tsutsui, K.; Matsui, T.; Kikuchi, R.; Eguchi, K. Catalytic abatement of acetaldehyde over oxide-supported precious metal catalysts. *Appl. Catal. B Environ.* **2008**, *78*, 158–165. [CrossRef]

121. Zhang, C.; He, H. A comparative study of TiO_2 supported noble metal catalysts for the oxidation of formaldehyde at room temperature. *Catal. Today* **2007**, *126*, 345–350. [CrossRef]

122. Zhang, C.B.; He, H.; Tanaka, K. Catalytic performance and mechanism of a Pt/TiO_2 catalyst for the oxidation of formaldehyde at room temperature. *Appl. Catal. B Environ.* **2006**, *65*, 37–43. [CrossRef]

123. Agarwal, S.K.; Spivey, J.J.; Butt, J.B. Catalyst deactivation during deep oxidation of chlorohydrocarbons. *Appl. Catal. A Gen.* **1992**, *82*, 259–275. [CrossRef]

124. Petrosius, S.C.; Drago, R.S.; Young, V.; Grunewald, G.C. Low-temperature decomposition of some halogenated hydrocarbons using metal oxide/porous carbon catalysts. *J. Am. Chem. Soc.* **1993**, *115*, 6131–6137. [CrossRef]

125. Sedjame, H.J.; Fontaine, C.; Lafaye, G.; Barbier, J.J. On the promoting effect of the addition of ceria to platinum based alumina catalysts for VOCs oxidation. *Appl. Catal. B Environ.* **2014**, *144*, 233–242. [CrossRef]

126. Carabineiro, S.; Chen, X.; Konsolakis, M.; Psarras, A.; Tavares, P.; Orf~ao, J.; Pereira, M.; Figueiredo, J. Catalytic oxidation of toluene on Ce-Co and La-Co mixed oxides synthesized by exotemplating and evaporation methods. *Catal. Today* **2015**, *244*, 161–171. [CrossRef]

127. Carabineiro, S.; Chen, X.; Martynyuk, O.; Bogdanchikova, N.; Avalos-Borja, M.; Pestryakov, A.; Tavares, P.; Orf~ao, J.; Pereira, M.; Figueiredo, J. Gold supported on metal oxides for volatile organic compounds total oxidation. *Catal. Today* **2015**, *244*, 103–114. [CrossRef]

128. Castano, M.H.; Molina, R.; Moreno, S. Catalytic oxidation of VOCs on $MnMgAlO_x$ mixed oxides obtained by auto-combustion. *J. Mol. Catal. A Chem.* **2015**, *398*, 358–367. [CrossRef]

129. Chen, H.; Zhang, H.; Yan, Y. Fabrication of porous copper/manganese binary oxides modified ZSM-5 membrane catalyst and potential application in the removal of VOCs. *Chem. Eng. J.* **2014**, *254*, 133–142. [CrossRef]

130. Solsona, B.; Davies, T.E.; Garcia, T.; Vázquez, I.; Dejoz, A.; Taylor, S.H. Total oxidation of propane using nanocrystalline cobalt oxide and supported cobalt oxide catalysts. *Appl. Catal. B Environ.* **2008**, *84*, 176–184. [CrossRef]

131. Liu, Q.; Wang, L.C.; Chen, M.; Cao, Y.; He, H.Y.; Fan, K.N. Dry citrate precursor synthesized nanocrystalline cobalt oxide as highly active catalyst for total oxidation of propane. *J. Catal.* **2009**, *263*, 104–113. [CrossRef]

132. Tseng, T.K.; Wang, L.; Ho, C.T.; Chu, H. The destruction of dichloroethane over a g-alumina supported manganese oxide catalyst. *J. Hazard. Mater.* **2010**, *178*, 1035–1040. [CrossRef]

133. Krishnamoorthy, S.; Rivas, J.A.; Amiridis, M.D. Catalytic oxidation of 1, 2-dichlorobenzene over supported transition metal oxides. *J. Catal.* **2000**, *193*, 264–272. [CrossRef]

134. Lahousse, C.; Bernier, A.; Grange, P.; Delmon, B.; Papaefthimiou, P.; Ioannides, T.; Verykios, X. Evaluation of g-MnO_2 as a VOC removal catalyst: Comparison with a noble metal catalyst. *J. Catal.* **1998**, *178*, 214–225. [CrossRef]

135. Parida, K.; Samal, A. Catalytic combustion of volatile organic compounds on Indian Ocean manganese nodules. *Appl. Catal. A Gen.* **1999**, *182*, 249–256. [CrossRef]

136. Luo, J.; Zhang, Q.; Huang, A.; Suib, S.L. Total oxidation of volatile organic compounds with hydrophobic cryptomelane-type octahedral molecular sieves. *Microporous Mesoporous Mater.* **2000**, *35–36*, 209–217. [CrossRef]

137. Aguero, F.N.; Scian, A.; Barbero, B.P.; Cadús, L.E. Influence of the support treatment on the behavior of MnO_x/Al_2O_3 catalysts used in VOC combustion. *Catal. Lett.* **2009**, *128*, 268–280. [CrossRef]

138. Kang, M.; Park, E.D.; Kim, J.M.; Yie, J.E. Manganese oxide catalysts for NOx reduction with NH3 at low temperatures. *Appl. Catal. A Gen.* **2007**, *327*, 261–269. [CrossRef]

139. Miranda, B.; Díaz, E.; Ordonez, S.; Vega, A.; Díez, F.V. Oxidation of trichloroethene over metal oxide catalysts: Kinetic studies and correlation with adsorption properties. *Chemosphere* **2007**, *66*, 1706–1715. [CrossRef]

140. Sun, H.; Liu, Z.; Chen, S.; Quan, X. The role of lattice oxygen on the activity and selectivity of the OMS-2 catalyst for the total oxidation of toluene. *Chem. Eng. J.* **2015**, *270*, 58–65. [CrossRef]

141. Cordi, E.M.; O'Neill, P.J.; Falconer, J.L. Transient oxidation of volatile organic compounds on a CuO/Al$_2$O$_3$ catalyst. *Appl. Catal. B Environ.* **1997**, *14*, 23–36. [CrossRef]

142. Hutchings, G.J.; Taylor, S.H. Designing oxidation catalysts. *Catal. Today* **1999**, *49*, 105–113. [CrossRef]

143. Heynderickx, P.M.; Thybaut, J.W.; Poelman, H.; Poelman, D.; Marin, G.B. The total oxidation of propane over supported Cu and Ce oxides: A comparison of single and binary metal oxides. *J. Catal.* **2010**, *272*, 109–120. [CrossRef]

144. Sinha, A.K.; Suzuki, K. Novel mesoporous chromium oxide for VOCs elimination. *Appl. Catal. B Environ.* **2007**, *70*, 417–422. [CrossRef]

145. Padilla, A.M.; Corella, J.; Toledo, J.M. Total oxidation of some chlorinated hydrocarbons with commercial chromia based catalysts. *Appl. Catal. B Environ.* **1999**, *22*, 107–121. [CrossRef]

146. Yim, S.D.; Chang, K.-H.; Nam, I.S. Deactivation of chromium oxide catalyst for the removal of perchloroethylene (PCE). *Stud. Surf. Sci. Catal.* **2001**, *139*, 173–180.

147. Gorte, R.J. Ceria in catalysis: From automotive applications to the water-gas shift reaction. *AlChE J.* **2010**, *56*, 1126–1135. [CrossRef]

148. Zimmer, P.; Tschope, A.; Birringer, R. Temperature-programmed reaction spectroscopy of ceria-and Cu/ceria-supported oxide catalyst. *J. Catal.* **2002**, *205*, 339–345. [CrossRef]

149. Huang, H.; Xu, Y.; Feng, Q.; Leung, D.Y.C. Low temperature catalytic oxidation of volatile organic compounds: A review. *Catal. Sci. Technol.* **2015**, *5*, 2649–2669. [CrossRef]

150. Li, H.; Lu, G.; Dai, Q.; Wang, Y.; Guo, Y.; Guo, Y. Hierarchical organization and catalytic activity of high-surface-area mesoporous ceria microspheres prepared via hydrothermal routes. *ACS Appl. Mater. Interfaces* **2010**, *2*, 838–846. [CrossRef]

151. Jones, J.; Ross, J.R. The development of supported vanadia catalysts for the combined catalytic removal of the oxides of nitrogen and of chlorinated hydrocarbons from flue gases. *Catal. Today* **1997**, *35*, 97–105. [CrossRef]

152. Delaigle, R.; Debecker, D.P.; Bertinchamps, F.; Gaigneaux, E.M. Revisiting the behaviour of vanadia-based catalysts in the abatement of (chloro)-aromatic pollutants: Towards an integrated understanding. *Top. Catal.* **2009**, *52*, 501–516. [CrossRef]

153. Solsona, B.; Garcia, T.; Aylon, E.; Dejoz, A.M.; Vazquez, I.; Agouram, S.; Davies, T.E.; Taylor, S.H. Promoting the activity and selectivity of high surface area Ni-Ce-O mixed oxides by gold deposition for VOC catalytic combustion. *Chem. Eng. J.* **2011**, *175*, 271–278. [CrossRef]

154. Delimaris, D.; Ioannides, T. VOC oxidation over MnO$_x$-CeO$_2$ catalysts prepared by a combustion method. *Appl. Catal. B Environ.* **2008**, *84*, 303–312. [CrossRef]

155. Morales, M.R.; Barbero, B.P.; Cadús, L.E. Total oxidation of ethanol and propane over Mn-Cu mixed oxide catalysts. *Appl. Catal. B Environ.* **2006**, *67*, 229–236. [CrossRef]

156. Vasile, A.; Bratan, V.; Hornoiu, C.; Caldararu, M.; Ionescu, N.I.; Yuzhakova, T.; Redey, A. Electrical and catalytic properties of cerium etin mixed oxides in CO depollution reaction. *Appl. Catal. B Environ.* **2013**, *140*, 25–31. [CrossRef]

157. Tang, W.; Wu, X.; Li, S.; Li, W.; Chen, Y. Porous Mn-Co mixed oxide nanorod as a novel catalyst with enhanced catalytic activity for removal of VOCs. *Catal. Commun.* **2014**, *56*, 134–138. [CrossRef]

158. Larsson, P.O.; Andersson, A. Complete oxidation of CO, ethanol, and ethyl acetate over copper oxide supported on titania and ceria modified titania. *J. Catal.* **1998**, *179*, 72–89. [CrossRef]

159. Hu, C.; Zhu, Q.; Jiang, Z.; Zhang, Y.; Wang, Y. Preparation and formation mechanism of mesoporous CuOeCeO2 mixed oxides with excellent catalytic performance for removal of VOCs. *Microporous Mesoporous Mater.* **2008**, *113*, 427–434. [CrossRef]

160. Delimaris, D.; Ioannides, T. VOC oxidation over CuO-CeO$_2$ catalysts prepared by a combustion method. *Appl. Catal. B Environ.* **2009**, *89*, 295–302. [CrossRef]

161. Rao, T.; Shen, M.; Jia, L.; Hao, J.; Wang, J. Oxidation of ethanol over Mn-Ce-O and Mn-Ce-Zr-O complex compounds synthesized by solegel method. *Catal. Commun.* **2007**, *8*, 1743–1747. [CrossRef]

162. Tang, X.; Li, Y.; Huang, X.; Xu, Y.; Zhu, H.; Wang, J.; Shen, W. MnO$_x$-CeO$_2$ mixed oxide catalysts for complete oxidation of formaldehyde: Effect of preparation method and calcination temperature. *Appl. Catal. B Environ.* **2006**, *62*, 265–273. [CrossRef]

163. Picasso, G.; Gutierrez, M.; Pina, M.; Herguido, J. Preparation and characterization of Ce-Zr and Ce-Mn based oxides for n-hexane combustion: Application to catalytic membrane reactors. *Chem. Eng. J.* **2007**, *126*, 119–130. [CrossRef]

164. Chen, H.; Sayari, A.; Adnot, A.; Larachi, F. Composition activity effects of Mn-Ce-O composites on phenol catalytic wet oxidation. *Appl. Catal. B Environ.* **2001**, *32*, 195–204. [CrossRef]

165. Yang, P.; Yang, S.; Shi, Z.; Meng, Z.; Zhou, R. Deep oxidation of chlorinated VOCs over CeO_2-based transition metal mixed oxide catalysts. *Appl. Catal. B Environ.* **2015**, *162*, 227–235. [CrossRef]

166. Li, J.; Zhao, P.; Liu, S. SnO_x-MnO_x-TiO_2 catalysts with high resistance to chlorine poisoning for low-temperature chlorobenzene oxidation. *Appl. Catal. A Gen.* **2014**, *482*, 363–369. [CrossRef]

167. Rao, G.R.; Sahu, H.R.; Mishra, B.G. Surface and catalytic properties of Cu-Ce-O composite oxides prepared by combustion method. *Coll. Surf. A Physicochem. Eng. Asp.* **2003**, *220*, 261–269. [CrossRef]

168. Jiang, X.; Lu, G.; Zhou, R.; Mao, J.; Chen, Y.; Zheng, X. Studies of pore structure, temperature-programmed reduction performance, and micro-structure of CuO/CeO_2 catalysts. *Appl. Surf. Sci.* **2001**, *173*, 208–220.

169. Zheng, X.C.; Wu, S.H.; Wang, S.P.; Wang, S.R.; Zhang, S.M.; Huang, W.P. The preparation and catalytic behavior of copperecerium oxide catalysts for low-temperature carbon monoxide oxidation. *Appl. Catal. A Gen.* **2005**, *283*, 217–223. [CrossRef]

170. Pecchi, G.; Reyes, P.; Zamora, R.; Cadus, L.E.; Fierro, J.L.G. Surface properties and performance for VOCs combustion of $LaFe_{1-y}Ni_yO_3$ perovskite oxides. *J. Solid State Chem.* **2008**, *181*, 905–912. [CrossRef]

171. Wei, T. Study on Catalytic Combustion of VOCs over Perovskite Catalysts. Master's Thesis, Zhejiang University of Technology, Zhejiang, China, 2005.

172. Beauchet, R.; Magnoux, P.; Mijoin, J. Catalytic oxidation of volatile organic compounds (VOCs) mixture (isopropanol/o-xylene) on zeolite catalysts. *Catal. Today* **2007**, *124*, 118–123. [CrossRef]

173. Rachapudi, R.; Chintawar, P.S.; Greene, H.L. Aging and Structure/Activity Characteristics of CR–ZSM-5 Catalysts during Exposure to Chlorinated VOCs. *J. Catal.* **1999**, *185*, 58–72. [CrossRef]

174. Muniandy, L.; Adam, F.; Mohamed, A.R.; Iqbal, A.; Rahman, N.R.A. Cu^{2+} coordinated graphitic carbon nitride (Cu-g-C_3N_4) nanosheets from melamine for the liquid phase hydroxylation of benzene and VOCs. *Appl. Surf. Sci.* **2017**, *398*, 43–55. [CrossRef]

175. Blanch-Raga, N.; Palomares, A.E.; Martínez-Triguero, J.; Valencia, S. Cu and Co modified beta zeolite catalysts for the trichloroethylene oxidation. *Appl. Catal. B Environ.* **2016**, *187*, 90–97. [CrossRef]

176. Lopez-Fonseca, R.; Aranzabal, A.; Steltenpohl, P.; Gutierrez-Ortiz, J.I.; Gonzalez Velasco, J.R. Performance of zeolites and product selectivity in the gas-phase oxidation of 1,2-dichloroethane. *Catal. Today* **2000**, *62*, 367–377. [CrossRef]

177. Kullavanijayam, E.; Trimm, D.L.; Cant, N.W. Adsocat: Adsorption/catalytic combustion for VOC and odour control. *Stud. Surf. Sci. Catal.* **2000**, *130*, 569–574.

178. Fujishima, A.; Honda, K. Electrochemical photolysis of water at a semiconductorelectrode. *Nature* **1972**, *238*, 37–38. [CrossRef] [PubMed]

179. Wang, D.; Hou, P.; Yang, P.; Cheng, X. $BiOBr@SiO_2$ flower-like nanospheres chemically-bonded on cement-based materials for photocatalysis. *Appl. Surf. Sci.* **2018**, *430*, 539–548. [CrossRef]

180. Li, Y.; Wu, X.; Li, J.; Wang, K.; Zhang, G. Z-scheme g-C3N4@CsxWO3 heterostructure as smart window coating for UV isolating, Vis penetrating, NIR shielding and full spectrum photocatalytic decomposing VOCs. *Appl. Catal. B Environ.* **2018**, *229*, 218–226. [CrossRef]

181. Mishra, A.; Mehta, A.; Kainth, S.; Basu, S. Effect of different plasmonic metals on photocatalytic degradation of volatile organic compounds (VOCs) by bentonite/M-TiO_2 nanocomposites, under UV/visible light. *Appl. Clay Sci.* **2018**, *153*, 144–153. [CrossRef]

182. Song, S.; Lu, C.; Wu, X.; Jiang, S.; Sun, C.; Le, Z. Strong base g-C_3N_4 with perfect structure for photocatalytically eliminating formaldehyde under visible-light irradiation. *Appl. Catal. B Environ.* **2018**, *227*, 145–152. [CrossRef]

183. Bhatkhande, D.S.; Pangarkar, V.G.; Beenackers, A.A.C.M. Photocatalytic degradation for environmental applications—A review. *J. Chem. Technol. Biotechnol. Int. Res. Process Environ. Clean Technol.* **2001**, *77*, 107–116. [CrossRef]

184. Choi, H.; Stathatos, E.; Dionysiou, D.D. Sol–gel preparation of mesoporous photocatalytic TiO_2 films and TiO_2/Al_2O_3 composite membranes for environmental applications. *Appl. Catal. B Environ.* **2006**, *63*, 60–67. [CrossRef]

185. Fujishima, A. TiO₂ photocatalysis and related surface phenomena. *Surf. Sci. Rep.* **2008**, *63*, 515–582. [CrossRef]

186. Minero, C. Surface modified photocatalysts, in environmental photochemistry part III. In *The Handbook of Environmental Chemistry*; Bahnemann, D.W., Robertson, K.J., Eds.; Springer: Berlin/Heidelberg, Germany, 2015; Volume 35, pp. 23–44.

187. Tejasvi, R.; Sharma, M.; Upadhyay, K. Passive photo-catalytic destruction of air-borne VOCs in high traffic areas using TiO₂-coated flexible PVC sheet. *Chem. Eng. J.* **2015**, *262*, 875–881. [CrossRef]

188. Li, F.B.; Li, X.Z.; Ao, C.H.; Lee, S.C.; Hou, M.F. Enhanced photocatalytic degradation of VOCs using Ln³⁺–TiO₂ catalysts for indoor air purification. *Chemosphere* **2005**, *59*, 787–800. [CrossRef]

189. Héqueta, V.; Raillarda, C.; Debonoa, O.; Thévenet, F.; Locoge, N.; Le Coq, L. Photocatalytic oxidation of VOCs at ppb level using a closed-loop reactor: The mixture effect. *Appl. Catal. B Environ.* **2018**, *226*, 473–486. [CrossRef]

190. Huang, L.; Nakajo, K.; Ozawa, S.; Matsuda, H. Decomposition of dichloromethane in a wire-in-tube pulsed corona reactor. *Environ. Sci. Technol.* **2001**, *35*, 1276–1281. [CrossRef]

191. Norberg, A. Modeling current pulse shape and energy in surface discharges. *IEEE Trans. Ind. Appl.* **1992**, *28*, 498–503. [CrossRef]

192. Rousseau, A.; Dantier, A.; Gatilova, L.; Ionikh, Y.; Röpcke, J.; Tolmachev, Y. On NOₓ production and volatile organic compound removal in a pulsed microwave discharge in air. *Plasma Sour. Sci. Technol.* **2005**, *14*, 70–75. [CrossRef]

193. Kogelschatz, U. Dielectric-barrier discharges: Their history, discharge physics, and industrial applications. *Plasma Chem. Plasma Process.* **2003**, *23*, 1–46. [CrossRef]

194. Yamamoto, T.; Ramanathan, K.; Lawless, P.A.; Ensor, D.S.; Newsome, J.R.; Plaks, N.; Ramsey, G.H. Control of volatile organic compounds by an ac energized ferroelectric pellet reactor and a pulsed corona reactor. *IEEE Trans. Ind. Appl.* **1992**, *28*, 528–534. [CrossRef]

195. Ding, H.-X.; Zhu, A.-M.; Yang, X.-F.; Li, C.-H.; Xu, Y. Removal of formaldehyde from gas streams via packed-bed dielectric barrier discharge plasmas. *J. Phys. D App. Phys.* **2005**, *38*, 4160–4167. [CrossRef]

196. Kim, H.H.; Ogata, A.; Futamura, S. Oxygen partial pressure-dependent behavior of various catalysts for the total oxidation of VOCs using cycled system of adsorption and oxygen plasma. *Appl. Catal. B Environ.* **2008**, *79*, 356–367. [CrossRef]

197. Futamura, S.; Yamamoto, T.; Lawless, P.A. Towards understanding of VOC decomposition mechanisms using nonthermal plasmas. In Proceedings of the 1995 Thirtieth IAS Annual Meeting IEEE Conference Record of Industry Applications Conference, Orlando, FL, USA, 8–12 October 1995; Volume 2, pp. 1453–1458.

198. Zheng, C.; Zhu, X.; Gao, X.; Liu, L.; Chang, Q.; Luo, Z.; Cen, K. Experimental study of acetone removal by packed-bed dielectric barrier discharge reactor. *J. Ind. Eng. Chem.* **2014**, *20*, 2761–2768. [CrossRef]

199. Lee, B.Y.; Park, S.H.; Lee, S.C.; Kang, M.; Choung, S.J. Decomposition of benzene by using a discharge plasma-photocatalyst hybrid system. *Catal. Today* **2004**, *93–95*, 769–776. [CrossRef]

200. Gandhi, M.S.; Ananth, A.; Mok, Y.S.; Song, J.I.; Park, K.H. Effect of porosity of α-alumina on non-thermal plasma decomposition of ethylene in a dielectric-packed bed reactor. *Res. Chem. Intermed.* **2014**, *40*, 1483–1493. [CrossRef]

201. Hu, J.; Jiang, N.; Li, J.; Shang, K.; Lu, N.; Wu, Y. Degradation of benzene by bipolar pulsed series surface/packed-bed discharge reactor over MnO₂-TiO₂/zeolite catalyst. *Chem. Eng. J.* **2016**, *293*, 216–224. [CrossRef]

202. Ogata, A.; Yamanouchi, K.; Mizuno, K.; Kushiyama, S.; Yamamoto, T. Oxidation of dilute benzene in an alumina hybrid plasma reactor at atmospheric pressure. *Plasma Chem. Plasma Process.* **1999**, *19*, 383–394. [CrossRef]

203. Zhu, X.; Gao, X.; Qin, R.; Zeng, Y.; Qu, R.; Zheng, C.; Tu, X. Plasma-catalytic removal of formaldehyde over Cu–Ce catalysts in a dielectric barrier discharge reactor. *Appl. Catal. B Environ.* **2015**, *170–171*, 293–300. [CrossRef]

204. Bradford, M.C.J.; Vannice, M.A. Estimation of CO heats of adsorption on metal surfaces from vibrational spectra. *Ind. Eng. Chem. Res.* **1996**, *35*, 3171–3178. [CrossRef]

205. An, H.T.Q.; Huu, T.P.; Le Van, T.; Cormier, J.M.; Khacef, A. Application of atmospheric non thermal plasma-catalysis hybrid system for air pollution control: Toluene removal. *Catal. Today* **2011**, *176*, 474–477.

206. Futamura, S.; Einaga, H.; Kabashima, H.; Hwan, L.Y. Synergistic effect of silent discharge plasma and catalysts on benzene decomposition. *Catal. Today* **2004**, *89*, 89–95. [CrossRef]

207. Wu, J.; Huang, Y.; Xia, Q.; Li, Z. Decomposition of toluene in a plasma catalysis system with NiO, MnO$_2$, CeO$_2$, Fe$_2$O$_3$, and CuO catalysts. *Plasma Chem. Plasma Process.* **2013**, *33*, 1073–1082. [CrossRef]

208. Zhao, D.-Z.; Li, X.-S.; Shi, C.; Fan, H.-Y.; Zhu, A.-M. Low-concentration formaldehyde removal from air using a cycled storage-discharge (CSD) plasma catalytic process. *Chem. Eng. Sci.* **2011**, *66*, 3922–3929. [CrossRef]

209. Ran, L.; Wang, Z.; Wang, X. The effect of Ce on catalytic decomposition of chlorinated methane over RuO$_x$ catalysts. *Appl. Catal. A gen.* **2014**, *470*, 442–450. [CrossRef]

210. Asilevi, P.J.; Yi, C.W.; Li, J.; Nawaz, M.I.; Wang, H.J.; Yin, L.; Junli, Z. Decomposition of formaldehyde in strong ionization non-thermal plasma at atmospheric pressure. *Int. J. Environ. Sci. Technol.* **2020**, *17*, 765–776. [CrossRef]

211. Zhu, T.; Li, J.; Jin, Y.; Liang, Y.; Ma, G. Decomposition of benzene by non-thermal plasma processing: Photocatalyst and ozone effect. *Int. J. Environ. Sci. Technol.* **2008**, *5*, 375–384. [CrossRef]

212. Urashima, K.; Kostov, K.G.; Chang, J.S.; Okayasu, Y.; Iwaizumi, T.; Yoshimura, K.; Kato, T. Removal of C$_2$F$_6$ from a semiconductor process flue gas by a ferroelectric packed-bed barrier discharge reactor with an adsorber. *IEEE Trans. Ind. Appl.* **2001**, *37*, 1456–1463. [CrossRef]

213. Ogata, A.; Ito, D.; Mizuno, K.; Kushiyama, S.; Gal, A.; Yamamoto, T. Effect of coexisting components on aromatic decomposition in a packed-bed plasma reactor. *Appl. Catal. A Gen.* **2002**, *236*, 9–15. [CrossRef]

214. Ogata, A.; Shintani, N.; Yamanouchi, K.; Mizuno, K.; Kushiyama, S.; Yamamoto, T. Effect of water vapor on benzene decomposition using a nonthermal-discharge plasma reactor. *Plasma Chem. Plasma Process.* **2000**, *20*, 453–467. [CrossRef]

215. Mustafa, M.F.; Fu, X.; Liu, Y.; Abbas, Y.; Wang, H.; Lu, W. Volatile organic compounds (VOCs) removal in non-thermal plasma double dielectric barrier discharge reactor. *J. Hazard. Mater.* **2018**, *347*, 317–324. [CrossRef] [PubMed]

216. Hirota, K.; Sakai, H.; Washio, M.; Kojima, T. Application of electron beams for the treatment of VOC streams. *Ind. Eng. Chem. Res.* **2004**, *43*, 1185–1191. [CrossRef]

217. Zimek, Z. High power accelerators and processing systems for environmental application. Radiation treatment of gaseous and liquid effluents for contaminant removal. *IAEA-TECDOC* **2005**, *1473*, 125–137.

218. Son, Y.S.; Kim, J.; Kim, J.C. Decomposition of acetaldehyde using an electron beam. *Plasma Chem. Plasma Process.* **2014**, *34*, 1233–1245. [CrossRef]

219. Son, Y.S.; Kim, K.H.; Kim, K.J.; Kim, J.C. Ammonia Decomposition Using Electron Beam. *Plasma Chem. Plasma Process.* **2013**, *33*, 617–629. [CrossRef]

220. Han, D.H.; Stuchinskaya, T.; Won, Y.S.; Park, W.S.; Lim, J.K. Oxidative decomposition of aromatic hydrocarbons by electron beam irradiation. *Radiat. Phys. Chem.* **2003**, *67*, 51–60. [CrossRef]

221. Hashimoto, S.; Hakoda, T.; Hirata, K.; Arai, H. Low energy electron beam treatment of VOCs. *Radiat. Phys. Chem.* **2000**, *57*, 485–488. [CrossRef]

222. Sun, Y.; Chmielewski, A.G.; Licki, J.; Bułka, S.; Zimek, Z. Decomposition of organic compounds in simulated industrial off-gas by using electron beam irradiation. *Radiat. Phys. Chem.* **2009**, *78*, 721–723. [CrossRef]

223. Son, Y.S.; Kim, P.; Park, J.H.; Kim, J.; Kim, J.C. Decomposition of trimethylamine by an electron beam. *Plasma Chem. Plasma Process.* **2013**, *33*, 1099–1109. [CrossRef]

224. Son, Y.S.; Park, J.H.; Kim, P.; Kim, J.C. Oxidation of gaseous styrene by electron beam irradiation. *Radiat. Phys. Chem.* **2012**, *81*, 686–692. [CrossRef]

225. Auslender, V.L.; Ryazantsev, A.A.; Spiridonov, G.A. The use of electron beam for solution of some ecological problems in pulp and paper industry. *Radiat. Phys. Chem.* **2002**, *63*, 641–645. [CrossRef]

226. Son, Y.S.; Kim, J.C. Decomposition of sulfur compounds by radiolysis: I. Influential factors. *Chem. Eng. J.* **2015**, *262*, 217–223. [CrossRef]

227. Son, Y.S.; Jung, I.H.; Lee, S.J.; Kim, J.C. Decomposition of sulfur compounds by a radiolysis: III. A hybrid system and field application. *Chem. Eng. J.* **2015**, *274*, 9–16. [CrossRef]

228. Son, Y.S.; Jung, I.H.; Lee, S.J.; Koutrakis, P.; Kim, J.C. Decomposition of sulfur compounds by radiolysis: II. By-products and mechanisms. *Chem. Eng. J.* **2015**, *269*, 27–34. [CrossRef]

229. Kim, J.C. Factors affecting aromatic VOC removal by electron beam treatment. *Radiat. Phys. Chem.* **2002**, *65*, 429–435. [CrossRef]